

**DETERMINATION OF EARTHQUAKE SOURCE PARAMETERS FOR THE
ELAZIĞ EARTHQUAKE OF MARCH 8, 2010 BASED ON SOURCE SPECTRA**

by

Tülay Yılmaz

B.S., Geophysical Engineering, Kocaeli University, 2006

Submitted to

Boğaziçi University

Kandilli Observatory and Earthquake Research Institute

in partial fulfillment of the requirements for the degree of Master of Science

Graduate Program in Geophysical Engineering

Boğaziçi University

2014

ACKNOWLEDGEMENTS

I would like to acknowledge the contributions of those who did not hesitate to help me in the writing process of this thesis. My heartfelt thanks go to the members of my thesis committee, especially Prof. Dr. Nurcan Meral Özel.

First of all, I would like to thank my supervisor Prof. Dr. Nurcan Meral Özel for agreeing to be my supervisor although she had already seven students. In addition, in the writing process of this thesis, she provided me with invaluable advice and criticisms which helped me give direction to my thesis. This thesis would not have been completed without her. She patiently reviewed innumerable drafts and contributed to all and every single process of the thesis. Second, my heartfelt thanks go to Ayşegül Köseoğlu and Mehmet Yılmaz who were very kind to me when I needed help in the process of analyzing the data, with which I had a lot of trouble.

I also would like to thank my parents, my brother Uğur Yılmaz and my future husband Emre Tepe who tried to make me feel self-confident and relaxed in this process.

I would particularly like to thank my friends and colleagues for their support and encouragement. Last, I would like to acknowledge the contributions of those who willingly took part in my study.

ABSTRACT

DETERMINATION OF EARTHQUAKE SOURCE PARAMETERS FOR THE ELAZIĞ EARTHQUAKE OF MARCH 8, 2010 BASED ON SOURCE SPECTRA

Elazığ province was experienced a moment magnitude of 6.0 ($M_w=6.0$) earthquake on March 8th, 2010 which was followed by a sequence of earthquakes ranging from moderate to large scale near the source of main shock, Başyurt-Karakoçan. Seismic source parameters and scaling relations were determined by using a data set of 29 earthquakes which were recorded by broadband seismic network whose epicentral distances vary between 10 - 600 km and magnitudes are ranging from 3.3 to 6.0 between March 8th and March 29th.

In this thesis, the source processes of these earthquakes are analyzed in terms of focal mechanism solutions, moment magnitude, seismic moment, corner frequency, stress drop and fault dimensions. Source parameters are computed by Moment Tensor Inversion method (MTI) represented by a point source model. Focal mechanism solutions are computed by using ZSACWIN software package (Yılmaz, 2011). Fault parameters (strike, dip, and rake angles), and seismic moment are calculated using the technique introduced by Dreger and Helmberger (1993), Dreger (2002). The focal mechanisms of 29 earthquakes are mostly strike-slip fault type, and the seismic moment of main shock determined as $M_0=7.21 \times 10^{24}$ dyne-cm.

The displacement source spectra are determined by applying ω^{-2} spectral fitting procedure to classical Brune's (1970) model using SEISAN software package (Ottemöller, 2011). The corrected spectra for S-waves within 5 sec are scaled to compute moment at the long period asymptote corresponding to the spectral plateau. Using the spectral amplitude (Ω_0) for 0 Hz, seismic moment (M_0) and corner frequency (f_c) which controls the shape of the spectra are derived from the fitted model based on the Brune's model by implementing Converging Grid Search (CGS) technique. The source dimension of a circular fault area, the average stress drop, and the M_w are calculated with respect to empirical relations proposed by Hanks and Kanamori (1979). For the mainshock of Elazığ earthquake, seismic

moment is calculated as $M_o = 1.80 \times 10^{25}$ dyne-cm in agreement with similar studies' results in the region and M_o from MTI method's results.

ÖZET

8 MART 2010 ELAZIĞ DEPREMİ'NİN KAYNAK PARAMETRELERİNİN KAYNAK SPEKTRUMUNA DAYALI OLARAK BELİRLENMESİ

Elazığ Bölgesi' nde 8 Mart 2010 tarihinde moment büyüklüğü $M_w=6.0$ olan ve anaşoku takiben deprem kaynağı ve civarında, Karakoçan-Başyurt yöresinde, orta ve büyük ölçekte artçı sarsıntılar meydana gelmiştir. 8 - 29 Mart 2010 zaman aralığında, geniş bant sismik istasyon ağı tarafından kaydedilen ve episantr uzaklıkları 10 - 600 km arasında değişen ve magnitüd değerleri 3.3 ile 6.0 arasında büyüklüğe sahip depremlerin sismik kaynak parametreleri belirlenmiştir.

Yapılan bu çalışmada, depremlerin kaynak bilgileri odak mekanizması çözümleri, moment magnitüdü, sismik momenti, köşe frekansının spektral düzeyi, stres düşümü, fay boyutları hesaplanarak analiz edilmiştir. Nokta kaynak tarafından temsil edilen kaynak parametreleri, Moment Tensör Ters Çözüm Yöntemi ile, odak mekanizması çözümleri ZSACWIN yazılım paketi (Yılmazer, 2011) kullanılarak hesaplanmıştır. Ters çözümden elde edilen fay parametreleri, fay geometrisi (doğrultu, eğim ve kayma yönü açıları) ve sismik moment Dreger and Helmberger (1993), Dreger (2002) tarafından tanımlanan yaklaşıma göre belirlenmiştir. 29 depremin odak mekanizması çoğunlukla doğrultu atımlı fay ve ana şokun sismik momenti $M_0 = 7.21 \times 10^{24}$ dyne-cm olarak tanımlanmıştır.

Yer değiştirme kaynak spektrumu, SEISAN yazılım paketi (Ottemöller, 2011) kullanılarak, Brune' un 1970 yılında tanımladığı ω^{-2} yerdeğiştirme spektrumu uyarlanarak elde edilmiştir. S dalgaları için hesaplanan yerdeğiştirme spektrumları, 5 saniyelik frekansa denk gelecek şekilde ölçeklendirilmiştir. Spektral genlik (Ω_0) '0' Hz için, sismik moment (M_0) ve kesme frekansı (f_c), yerdeğiştirme spektrumu yakınsak tarama (yakınsama grid araştırma) yöntemi kullanılarak, Brune'un kaynak modeline uyarlanarak elde edilmiştir. Dairesel bir fay alanı üzerindeki kaynak boyutu, ortalama stres düşümü ve Moment magnitüd Hanks and Kanamori (1979) tarafından tanımlanan ampirik ilişkiler ile bağıntılar kullanılarak hesaplanmıştır. Elazığ depreminin sismik momenti, $M_0 = 1.80 \times 10^{25}$ dyne-cm

olarak bulunmuş ve bu sonuç MTI yöntemin sonuçlarından elde edilen sonuçlarla ve yayınlanan sonuçlarla uyumlu olduğu gösterilmiştir.

TABLE OF CONTENTS

ACKNOWLEDGEMENTS	iii
ABSTRACT	iv
ÖZET	vi
LIST OF FIGURES	x
LIST OF TABLES	xiii
LIST OF SYMBOLS	xv
LIST OF ABBREVIATES	xvi
1. INTRODUCTION	1
2. METHODOLOGY	8
2.1. SEISAN Software	8
2.1.1. General Definitions (For Determination of Source Parameters Using Displacement Spectra)	8
2.1.1.1. Source Spectrum and Source Parameters	9
2.1.1.2. Geometrical Spreading, $G(R)$	9
2.1.1.3. Diminution Function, $D(f)$	10
2.1.1.4. Q Absorption	11
2.1.1.5. κ Near Surface Attenuation	12
2.1.1.6. Source Spectrum	12
2.1.2. General Structure of SEISAN	13
2.1.2.1. Wav Directory (Waveform File Directory)	14
2.1.2.2. Rea Directory	16
2.1.2.3. Cal Directory (Response File Directory)	16

2.1.3. Definition Files	18
2.2. ZSACWIN Software	18
2.2.1. Layout of ZSACWIN Software on Computer	19
2.2.2. Overall Program Flow, Function Capacity	20
3. DATA PROCESSING	21
3.1. Processing with SEISAN	22
3.2. Processing with ZSACWIN	24
3.2.1. Generalized Processing Structure of ZSacWin	24
3.2.2. Determination of Epicenter and Origin Time of Earthquakes	26
3.2.3. Determining Magnitude of an Earthquake	26
3.2.3.1. Local Magnitude	26
3.2.4. Determination of Faulting Parameters Using MTI	27
4. RESULTS	30
5. CONCLUSIONS	42
6. REFERENCES	46

LIST OF FIGURES

<p>Figure 1.1. The general map shows the main fault systems in and around Turkey (modified from Barka and Kadinsky-Cade, 1988; Saroglu <i>et al.</i>, 1992; Koçyiğit and Beyhan, 1998; Okay <i>et al.</i>, 2000). The black thick arrows indicate relative plate motions. The detailed map of the EAFZ region displays segments, sampling sites, and the main seismic events (modified from Perinçek <i>et al.</i>, 1987; Kozlu, 1987; Perinçek and Çemen, 1990; Saroglu <i>et al.</i>, 1992; Aksu <i>et al.</i>, 1992). NAFZ: North Anatolian Fault Zone; EAFZ: East Anatolian Fault Zone; EFZ: Ecemiş Fault Zone; BSZ: Bitlis Suture Zone. The black dots indicate the epicentral areas for the shocks detailed in the squared labels with magnitude and date. Squared marks = sampling site labels = collected samples. Blackfilled circles = EAFZ segments; segment numbers: 1—Karlıova-Bingöl segment; 2—Palu–Lake Hazar segment; 3—Lake Hazar–Sincik segment; 4—Çelikhan–Erkenek segment; 5—Gölbaşı–Türkoğlu segment; 6—Türkoğlu–Antakya segment</p>	1
<p>Figure 1.2. The distribution of the large earthquakes occurred in the region within the last century (from KOERI, March 2010)</p>	3
<p>Figure 1.3. The distribution of the aftershocks. (Red star is main shock, blue star is second large shock, purple circles are the earthquakes with magnitude, M=4.0-4.9 (from KOERI, March 2010)</p>	4
<p>Figure 1.4. Computed Fault mechanism of the mainshock from Moment Tensor Inversion solutions</p>	4
<p>Figure 2.1. Structure of SEISAN (Ottemöller <i>et al.</i>, 2011)</p>	13

Figure 3.1. Map of the used seismic stations in the study. The figure was created by ZSacWin Analysis Software Package (Yilmazer, 2011)	21
Figure 3.2. Flow diagram related to main functions of the software	25
Figure 3.3. MTI results for 2010.08.03 07:47:38 Elazığ- Kovancılar earthquake	29
Figure 4.1. Examples of displacement source spectra obtained for event #1 (see Table 4.1) The blue line presents the original displacement spectra; the red line indicates the synthetic spectra resulted from the automatic procedure; the green line at the bottom signs the noise spectra	32
Figure 4.2. Examples of displacement source spectra for event #10 (see Table 4.1) The blue line presents the original displacement spectra; the red line indicates the synthetic spectra resulted from the automatic procedure; the green line at the bottom signs the noise spectra	33
Figure 4.3. Examples of displacement source spectra for event #29 (see Table 4.1) The blue line presents the original displacement spectra; the red line indicates the synthetic spectra resulted from the automatic procedure; the green line at the bottom signs the noise spectra	34
Figure 4.4. Comparison of the M_W results versus M_L results taken by the KOERI's catalogue	35
Figure 4.5. Comparison of the estimated parameters with the scalings Moment Magnitude of as a function of corner frequency	36
Figure 4.6. The estimated parameters based on source radius as a function of seismic moment	37

Figure 4.7. Examples of MTI method using ZSACWin software package obtained from 19 stations for event #1 (see Table 4.1)	39
Figure 4.8. M_w^{MTI} versus M_w^{SPEC}	40

LIST OF TABLES

Table 1.1. The number of damaged buildings and casualties in preliminary EQs occurred in the region (from KOERI, March 2010)	2
Table 2.1. The Structure of SEISAN contains the following main subdirectories	14
Table 2.2. An example of generating a SEISAN format using WAVETOOL	15
Table 2.3. A Typical S-file	16
Table 2.4. An example of GSE response file generated by RESP for the SEISAN	17
Table 2.5. An example of GSE response file generated by RESP for the SEISAN	18
Table 2.6. Sub index and files which are stored in the main folder	19
Table 3.1. Velocity structure ($V_p/V_s=1.73$)	24
Table 3.2. Relations between scalar moment tensor components (M_{ij}), seismic moment (M_o) and faulting components (strike, dip and rake)	28
Table 4.1. Estimated source parameters of 29 earthquakes which are given with their mean values and standard deviations. In order, N: event ID, Date: year, month, day, Hour: hour and minutes of origin time (UTC), h: depth (km), M_L : the Richter magnitude, M_w : the mean value of stations moment magnitude, Std: standard deviation of given value, M_o : seismic moment (dyne-cm), σ : stress drop in bars, f_c : corner frequency, α : source radius in km, GAP: maximum azimuthal gap between stations used in location, NS: number of stations used in solutions, respectively	31

Table 4.2. Obtained source fault parameters and seismic moment with using MTI method.	38
Table 4.3. Comparison of both M_w values obtained from displacement spectra and MTI method	41

LIST OF SYMBOLS

M_w	: Moment Magnitude
M_L	: The Richter magnitude
M_o	: Seismic Moment (dyne-cm)
Ω	: Spectral level (ms)
f	: Frequency (Hz)
f_c	: Corner frequency (Hz)
h	: Depth (km)
α	: Source radius (km)
Q	: The quality factor
κ	: Near surface attenuation
ρ	: Density (gr/cm^3)
v_s	: S wave velocity (km/s)
VR	: Variance Reduction
μ	: Rigidity (dyne/cm^2)
σ	: Stress Drop (bar)
S/N	: Signal/Noise

LIST OF ABBREVIATES

AGRB	: Ağrı Station
BAYT	: Bayburt Station
BNN	: Bünyan Station
BSZ	: Bitlis Suture Zone
CAL	: System Calibration Files
CGS	: Converging Grid Search
CMT	: Centroid Moment Tensor
DAT	: Default and Parameters Files
DYBB	: Diyarbakır Station
EAFZ	: East Anatolian Fault Zone
EFZ	: Ecemiş Fault Zone
ERD	: Earthquake Research Department
EW	: Earthworm
FFT	: Fast Fourier Transform
GSE	: Group of Scientific Experts
ILIC	: İliç – Erzincan Station
KOERI	: Kandilli Observatory and Earthquake Research Institute
NAFZ	: North Anatolian Fault Zone
NEMC	: National Earthquake Monitoring Centre

MAZI	: Mazıdağı – Mardin Station
MALT	: Malatya - Station
MTI	: Moment Tensor Inversion
PTK	: Petek – Tunceli Station
REA	: Earthquake Readings and Full Epicenter Solutions in a Database
RESP	: Instrument Response Files
SAC	: Seismic Analysis Code
SEISAN	: The Earthquake Analysis Software
SEISMO	: The Main Directory
TÜBİTAK	: Türkiye Bilimsel ve Teknolojik Araştırma Kurumu
WAV	: Waveform File Directory
ZSACWIN	: The Earthquake Analysis Software

1. INTRODUCTION

The East Anatolian Fault System is one of the most active fault systems in Turkey. The EAFS is approximately 30 km wide, 700 km long and a N–E trending sinistral mega shear zone between Anatolian plate in the north and African–Arabian plates in the south (İnceöz *et al.*, 2006). Because of the northward movement of Arabian and African plates, the Anatolian Block has a westward extrusion as shown in Figure 1.1a (Yılmaz *et al.*, 2006). Since EAF serves as a belt between two plates, the region of East Anatolia is acknowledged as a seismically very active (Arpat and Saroğlu, 1972). The system has produced numerous earthquakes which are a spatial distributed in the region (shown in Figure 1.1b) within the last century. As a significant seismic event that the region experienced within the last decade, was the 2003 $M_w=6.4$ Bingöl earthquake causing 176 fatalities and 520 injuries (Aydan *et al.*, 2003).

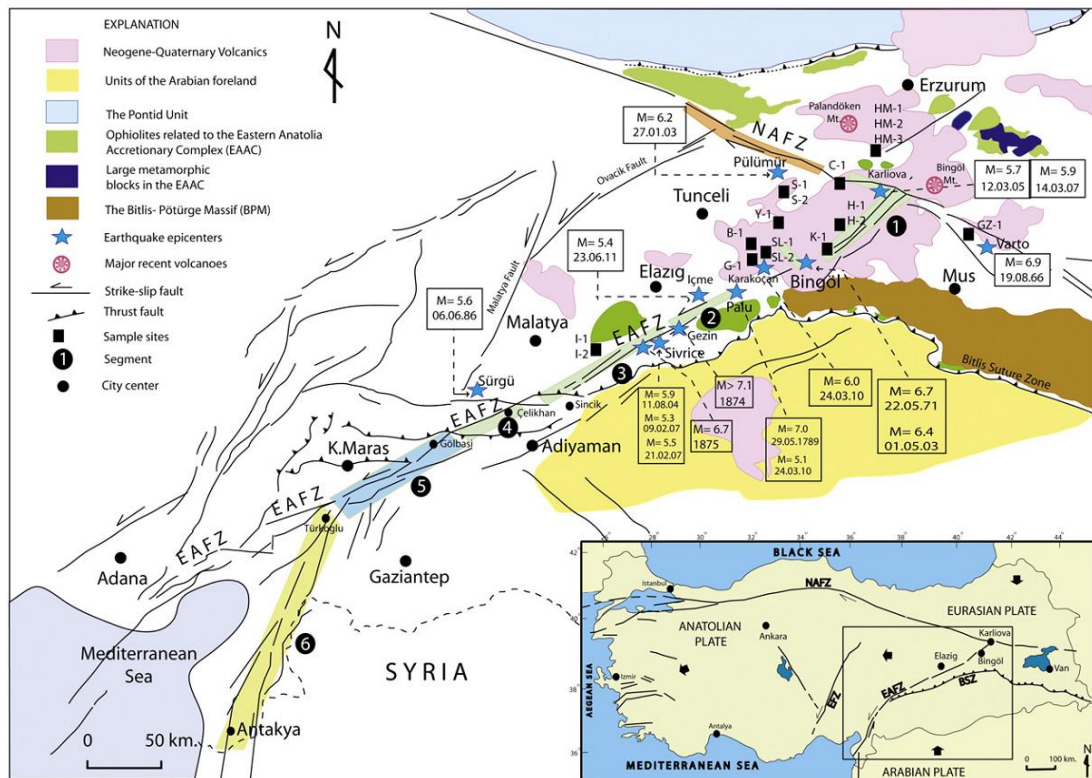


Figure 1.1. The general map shows the main fault systems in and around Turkey (modified from Barka and Kadinsky-Cade, 1988; Saroğlu *et al.*, 1992; Koçyiğit and

Beyhan, 1998; Okay *et al.*, 2000). The black thick arrows indicate relative plate motions.

The detailed map of the EAFZ region displays segments, sampling sites, and the main seismic events (modified from Perinçek *et al.*, 1987; Kozlu, 1987; Perinçek and Çemen, 1990; Saroğlu *et al.*, 1992; Aksu *et al.*, 1992). NAFZ: North Anatolian Fault Zone; EAFZ: East Anatolian Fault Zone; EFZ: Ecemiş Fault Zone; BSZ: Bitlis Suture Zone. The black dots indicate the epicentral areas for the shocks detailed in the squared labels with magnitude and date. Squared marks = sampling site labels = collected samples. Blackfilled circles = EAFZ segments; segment numbers: 1—Karlıova-Bingöl segment; 2—Palu–Lake Hazar segment; 3—Lake Hazar–Sincik segment; 4—Çelikhan–Erkenek segment; 5—Gölbaşı–Türkoğlu segment; 6—Türkoğlu–Antakya segment.

The faults are seismically active and form the source for many earthquakes. Some of the major earthquakes in the 20th Century are 13 September 1924 Pasinler (M = 6.8), 1975 Lice (M = 6.6), 24 November 1976 Çaldıran (M = 7.3), 30 October 1983 Horasan–Narman (M = 6.8), 5 May 1986 (M = 5.8) and 6 June 1986 Doğanşehir (M = 5.6) earthquakes (Bozkurt, 2001). The most destructive earthquake on the EAFZ is the 1971 Bingöl earthquake of $M_s = 6.8$ whose epicenter was near Bingöl (Kutunis *et al.*, 2010).

Table 1.1. The number of damaged buildings and casualties in preliminary EQs occurred in the region (from KOERI, March 2010).

Year	Earthquakes	Magnitude (Ms)	The number of damaged buildings	The number of casualties	The number of damaged buildings / The number of casualties
2003	The Bingöl Earthquake	Ms 6.4	1602	177	9.1
1983	Erzurum -Kars Earthquake	Ms 7.1	3240	1400	2.3
1976	Caldıran - Muradiye Earthquake	Ms 7.5	9232	3840	2.4
1971	The Bingöl Earthquake	Ms 6.8	5000	755	6.6
1943	The Corum Earthquake	Ms 7.2	2554	618	4.1
1939	The Erzincan Earthquake	Ms 7.9	116720	32968	3.5

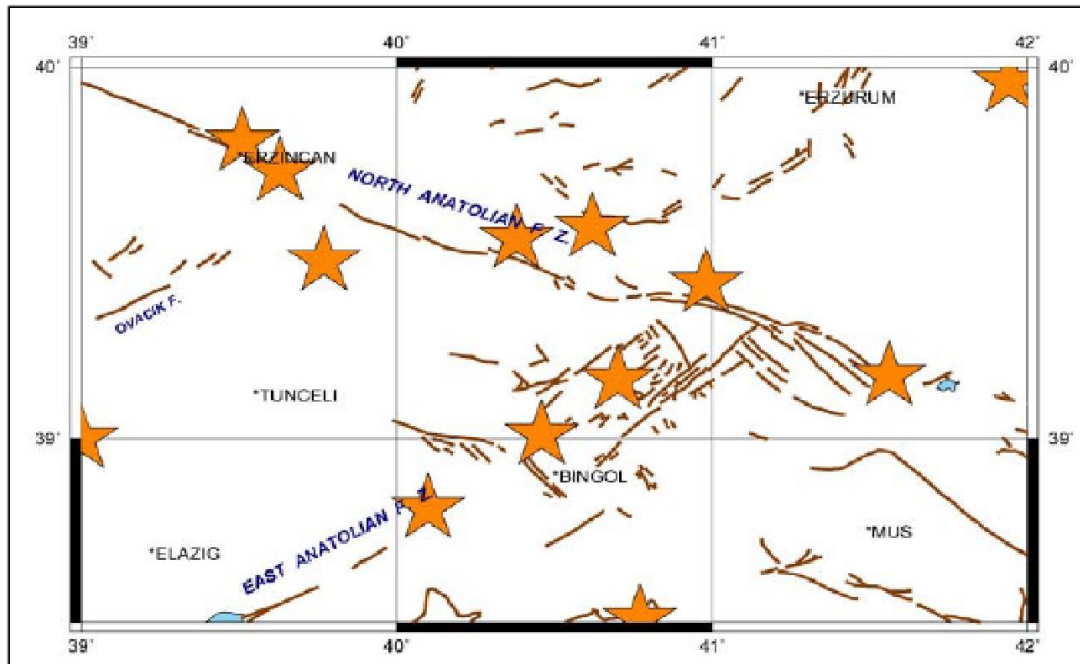


Figure 1.2. The distribution of the large earthquakes occurred in the region within the last century (from KOERI, March 2010).

The Elazığ earthquake of March 8, 2010, which is studied in this research, is centered in the field of Başyurt-Karakoçan, Elazığ. The mainshock took place at 04:32 local time with an approximated magnitude of 6.0. While impacts of the Earthquake were mainly concentrated on Kovancılar, Başyurt, Karakoçan, Gökdere districts in Elazığ, minor losses were observed in Erzincan, Batman, Tunceli, Malatya, Bingöl, Diyarbakır provinces (KOERI, March 2010). Earthquake Research Department (ERD) reported the epicenter of the Elazığ earthquake as 38.7752N - 40.0295E and with a depth of 5 km. The earthquake was reported as the left lateral strike slip East Anatolian Fault (EAF) which is consistent with the distribution of the aftershocks (TÜBİTAK MAM Report, 2010).

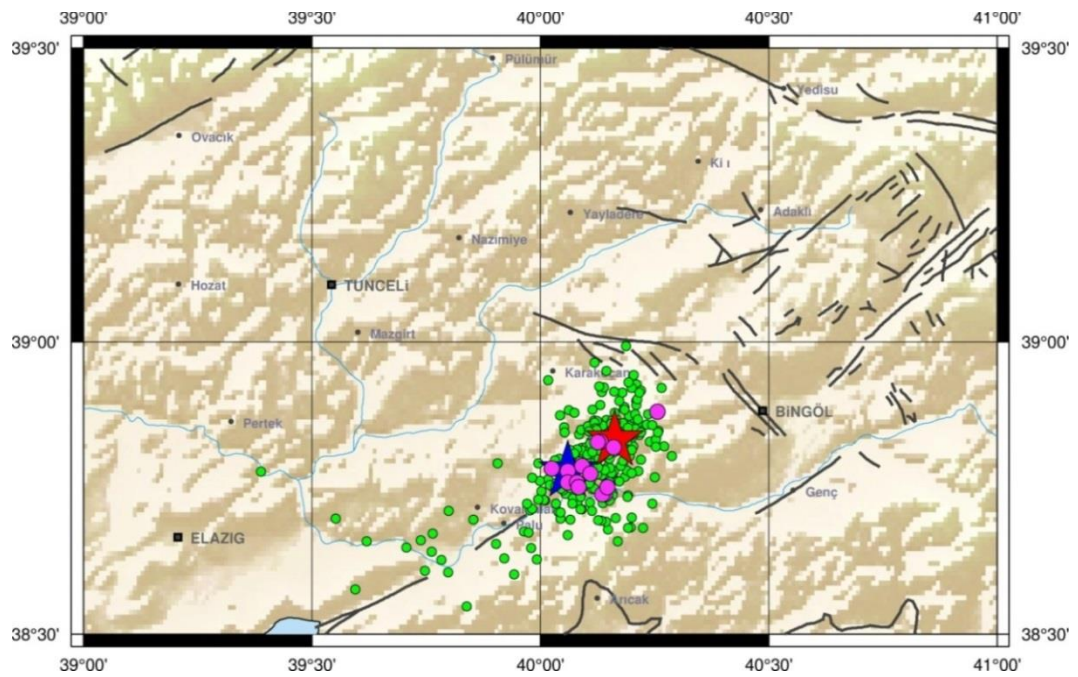


Figure 1.3. The distribution of the aftershocks. (Red star is main shock, blue star is second large shock, purple circles are the earthquakes with magnitude, $M=4.0-4.9$ (from KOERI, March 2010).

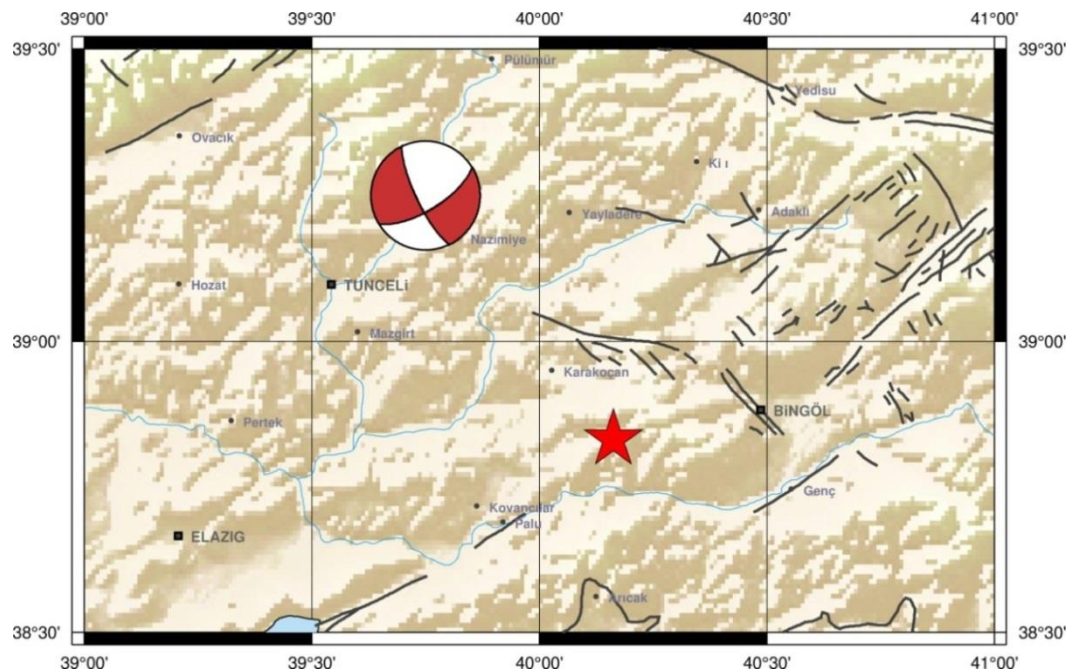


Figure 1.4. Computed Fault mechanism of the mainshock from Moment Tensor Inversion solutions.

Tan *et al.* (2011) reported that aftershock depths indicate a seismogenic brittle zone of about 15 km deep and stress changes which are as a result of the event potentially load on the segments more than 0.5 bar of stress on the NE end of the Palu segment and the SW end of the Göynük segment. Finally, they indicate that this earthquake has a compressional axis on the strike of 54° , dip with 80° and rake angle of -10° .

According to the study of Baykal *et al.* (2012), The 2010 Elazığ-Kovancılar earthquake is characterized by shallow depth rupture with high stress drop. General characteristic of entire EAFZ is indicated by left-lateral strike slip faulting. Moment Tensor solutions confirmed such kind of faulting. According to the Centroid Moment Tensor (CMT) solution of the Global CMT Project, this earthquake has a compressional axis on the strike of 228° , dip with 83° and rake angle of -21° .

Çubuk *et al.* (2011) concluded that this earthquake shows left-lateral strike slip faulting with a focal depth of 6 km. Strike, dip and rake angles are determined as 48° , 79° and 2° , respectively. They also found that seismic moment of the earthquake (M_0) is 7.81×10^{24} dyne-cm, moment magnitude (M_w) is 5.9, and the rupture time is approximately 3s.

The source parameters especially moment magnitude have a significant role in the estimation of attenuation relationships in the earthquake scenario studies, determination of the source parameter scaling relationships, prediction of the seismic hazard for the region. An earthquake of $M_w=6.1$ occurred on 8 march 2010 in Elazığ and Kovancılar and in this thesis the source parameters of mainshock and followed aftershocks have been estimated. The main purpose of this study is to search the earthquake by calculating source parameters of the Elazığ earthquake main shock and aftershocks. In this direction, two different methods; MTI and displacement spectra are used.

As a first step, earthquake data for the area were retrieved from KOERI database. P and S phases, are used to compute source parameters of the earthquake by using both software (ZSACWin and SEISAN). In both methods, the velocity model is defined based on the model which was introduced by; Kalafat (1987) and Kalafat *et al.* (1992). In both methods, minimization of difference between theoretical and observational arrival times is defined as the basic approach.

The velocity records are converted from time to frequency domain by implementing the formal fast fourier transform. The displacement source spectra are determined by applying ω^{-2} spectral fitting procedure to classical Brune's (1970) model using SEISAN software package. Together with previously computed parameters and use of relevant thresholds, stress drop, earthquake radius and moment magnitude that belong to the earthquake are calculated. In order to verify the reliability of these calculations, all these parameters are also manually calculated to compare with software outputs. After obtaining the same result on both methods, Converging Grid Search (CGS) method is verified. In the calculation procedure, almost all source parameters of the Elazığ main shock and aftershocks are obtained.

Moment Tensor Inversion (MTI) calculations as a second inversion method which are computed in time domain are applied by using ZSACWIN software. Focal mechanism solutions are computed by using ZSACWIN software package. Obtained fault parameters from the inversion are fault geometry (strike, dip, and rake angles) and seismic moment which are calculated according to the technique introduced by Dreger and Helmberger (1993), Dreger (2002).

According to our computation of the main shock parameters using displacement spectra method, seismic moment and moment magnitude are estimated as $M_0=1.80 \times 10^{25}$ dyne-cm, $M_w=6.0$ respectively. Also, in this study, we used MTI as an alternative method. According to the MTI method, the focal mechanism of investigated 29 earthquakes are mostly identified as strike-slip fault type and the main shock parameters which are seismic moment, moment magnitude and depth are computed as $M_0= 7.21 \times 10^{24}$ dyne-cm, $M_w=5.9$, and $h=12$ km, respectively. In addition to our previous findings, we also estimated that the main shock has a compressional axis of the strike of 58.55° , dip 68.03° , and rake angle of -14.80° by using MTI method. Finally, we concluded that our results for the 2010 Elazığ earthquake are similar to findings of other studies which are conducted in the region by different agencies.

Çubuk *et al.* (2011) obtained that this earthquake shows left-lateral strike slip faulting with a focal depth of 6 km. They also found that seismic moment of the earthquake (M_0) is $7,81 \times 10^{24}$ dyne-cm, moment magnitude (M_w) is 5.9. Tan *et al.* (2011) found that aftershock depths indicate a seismogenic brittle zone of about 15 km depth and

they computed that this earthquake's moment magnitude (M_w) is 6.1. According to the study of Baykal *et al.* (2012), The 2010 Elazığ-Kovancılar earthquake is characterized by shallow depth rupture with high stress drop. General characteristic of whole EAFZ is indicated by left-lateral strike slip faulting.

According to finding of the Global CMT Project based on the CMT method, this earthquake has a compressional axis on the strike of 228° , dip with 83° and rake angle of -21° . In addition, according to Fault parameters obtained by Tan *et al.* (2011), this earthquake has a compressional axis on the strike of 54° , dip with 80° , and rake angle of -10° . Finally, Strike, dip and rake angles were determined as 48° , 79° and 2° , respectively by Çubuk *et al.* (2011).

2. METHODOLOGY

In the section, brief information about used software for calculation of source parameters is presented.

2.1. SEISAN Software

The SEISAN (The Earthquake Analysis Software) seismic analysis system is a complete set of programs and a simple database for analyzing earthquakes from analog and digital data. With SEISAN, it is possible to use local and global earthquakes to enter phase readings manually or pick them with a cursor, locate events, edit events, determine spectral parameters, seismic moment, azimuth of arrival from 3-component stations and plot epicenters.

The SEISAN binary format is used in the seismic analysis program SEISAN and other programs (<ftp://ftp.geo.uib.no/pub/seismo/SOFTWARE/SEISAN/>). The format consists of a main header describing all channels. Each channel follows with a header that includes basic information response. SEISAN can read binary SEISAN files written on any platform, as well as SEED, MiniSEED, GSE and SAC. Since the data comes in one block per channel with time stamp only on the first sample, it is assumed that there are no time gaps. If there is more than one channel in the file, they arrive one after each other. Data files are limited with respect to the size, usually not more than a few hours. There is no built in compression. A channel can be read through direct access.

2.1.1. General Definitions (For Determination of Source Parameters Using Displacement Spectra)

Signal, monitored by seismograph, are affected by several factors on the way from source to receiver. In general, these impacts are varied based on wave attenuation, near surface attenuation and geometric spreading which depend on physical parameters of the ground between the source and the receiver. Real ground movement depends on waves

imposed by radiation pattern, local conditions and attenuation on the way between the source and the receiver. All these factors play importance in recording earthquake and dimension of spectra. Therefore, these impacts should be carefully defined.

2.1.1.1. Source Spectrum and Source Parameters. The displacement spectral amplitude $A(f)$, after removal of the instrument response $I(R)$ is given by the Equation (2.1) (Ottemöller and Havskov, 2003).

$$A(f)=S(f).D(f).G(R) \quad (2.1)$$

Where,

$A(f)$ = Spectral amplitude

$S(f)$ = Source function

$D(f)$ =Diminution function

$G(R)$ =Geometrical Spreading

$I(R)$ = Instrument Response

A signal which is recorded at velocity domain is determined by Equation (2.1).

Where R is the hypocentral distance, $S(f)$ is the source term, $D(f)$ is the diminution function, $G(R)$ is the geometrical spreading and $I(R)$ is the instrument response. Equation (2.1) is valid for both P and S/Lg waves with different $S(f)$, $D(f)$, and $G(R)$ terms for the respective wave types.

2.1.1.2. Geometrical Spreading, $G(R)$. Geometrical spreading is dependent on the wave type and the distance. We are describing it with the function $G(R)$.

Equation (2.2) assumes a constant type of geometrical spreading independent of hypocentral distance. For S-waves, body waves are often assumed for the near field and surface waves for larger distances under the assumption that the S-waves are dominated by Lg waves and commonly written as the Hermann and Kijko, (1980) relation.

$$\text{For P waves, } G(R) \qquad G(R) = 1/R \qquad (2.2)$$

$$\text{For S, Lg waves, } G(R) \qquad G(R)=1/R \qquad R \leq 100 \text{ km} \qquad (2.3)$$

$$G(R) = 1/(100R)^{1/2} \qquad R \geq 100 \text{ km}$$

These equations are valid for earthquake occurs at depths smaller than 50 km. In Elazığ earthquake, main shock and aftershocks mostly occurred at about 5 km depth and the equation given in 2.3 is appropriate to use.

2.1.1.3. Diminution Function, D(f). Ground movements recorded on surface of the earth are different from recorded movements underground in terms of amplitude and frequency (Tucker and *et al.*, 1984; Abercrombie, 1997). Factors have an impact on spectral shape of seismic waves that provide significant information on defining earthquake records.

Diminution function which is described in Equation (2.4) is one of these factors. Seismic waves are absorbed while traveling from focus of earthquake to the receiver on the earth.

The diminution function D(f) consists of two parts;

$$D(f)=P(f).N(f) \qquad (2.4)$$

where, N(f) accounts for near surface losses, P(f) accounts for losses along the travel path.

$$P(f)=\exp[(-\pi Tf)/Q(f)] \qquad (2.5)$$

Where, T is the travel time, which for Lg and surface waves is given by R/Vg with the hypocentral distance R and the group velocity Vg.

The effect of absorption on the spectral shape at local distances is indicated as Q value while the effect of absorption in shallow depth is labelled as κ (the near surface attenuation). Q parameter is frequency-dependent. Elimination of the effect of attenuation on spectrum is very important to define corner frequency and also source parameters.

To obtain the source term $S(f)$, elimination of radiation effect is required. In this sense, the signal is firstly converted from velocity to the displacement and instrument effects $I(R)$ have been removed.

2.1.1.4. Q Absorption. Q has been observed to have strong regional variation in the lithosphere while it is more stable in the interior of the earth. Q in the lithosphere is most often observed to have a frequency dependency of the form.

$$1 < f < 2 \rightarrow Q_{\beta}/Q_{\alpha} > 1 \text{ Hz} \quad (2.6)$$

$$f < 1 \rightarrow Q_{\beta}/Q_{\alpha} \sim 0.5 \text{ Hz}$$

$Q(f) = Q(f)$ is the frequency-dependent quality factor, often given in the simple form of (e.g., Aki, 1980).

when $f > 1 \text{ Hz}$,

$$Q(f) = Q_0 \cdot f^{\alpha} \quad (2.7)$$

Q_{α} for P waves, Q_{β} for S waves

There is some discussion on the values of Q for $f < 1 \text{ Hz}$ where some studies claim that the factor starts increasing again between $0.1 \text{ Hz} < f < 1 \text{ Hz}$, however the dominant view is that Q is constant for $0.1 \text{ Hz} < f < 1 \text{ Hz}$, see e.g. Stein and Wysession (2003).

For spectral analysis at regional distances, the effect of Q is small at low frequencies. The amplitude decay caused by Q is due to two mechanisms: Intrinsic Q due to heat loss (also called seismic absorption) and the redistribution of energy due to scattering.

In the study, $Q_0=35$ and $f^\alpha=0,83$ are used for the region (Eyidoğan *et al.*, 1999).

$$Q_s(f)=35*f^{0.83} \quad (2.7a)$$

It is expected that Q parameters are different for P and S waves.

2.1.1.5. κ Near Surface Attenuation. The term $N(f)$ accounts for the near-surface losses where κ depends on the quality factor in the near-surface layers.

$$N(f)=\exp(-\pi\kappa f) \quad (2.8)$$

The correction of $N(f)$ is especially influential for near surface layers which are directly affected by κ factor (Singh *et al.*, 1982). The correction for $N(f)$ is not applied in the analysis under scope of this study, since there is no consensus on the quality factor $N(f)$ for the region among researchers. This correction of $N(f)$ in displacement spectra method is necessary for any earthquake with a magnitude smaller than 3.0, however we excluded any earthquake less than 3.3 magnitude in this study (Küsmezer, *et al.*, 2010). Therefore, the correction of $N(f)$ is not applied into our analysis procedure.

2.1.1.6. Source Spectrum. $S(f)$ source function can be finally obtained after applying abovementioned corrections.

The source term for a simple ω^{-2} model is given by (Aki, 1967; Brune, 1970, 1971) the Equation (2.9).

$$S(f) = \frac{M_0}{4\pi\rho\kappa v^3} * \left[1 + \frac{f^2}{f_c^2}\right]^{-1} \quad (2.9)$$

ρ =density (kg/m^3), V is either the P or S-wave velocity at the source, M_0 =seismic moment (dyne-cm), f_c = corner frequency, f =frequency, $k=1/(2.0 \times 0.6)^{1/2} = 0.83$ is a factor to correct for free-surface reflection and f_c is the corner frequency.

The moment magnitude was defined by Hanks and Kanamori (1979) through the linear relation of energy and magnitude. The M_w scale is given by

$$M_w = 2/3 \log_{10} M_0 - 10.73 \quad (2.10)$$

where, M_0 is given in dyne-cm.

The source parameters are calculated by adapting amplitude spectrum to theoretical Brune's source model. Moment magnitude M_w is calculated by using Equation (2.10).

2.1.2. General Structure of SEISAN

The entire SEISAN system is located in subdirectories residing under the main directory SEISMO. Table 2.1 shows the structure of SEISAN. SEISAN contains many tools for converging data from one format to another and to import and export data.

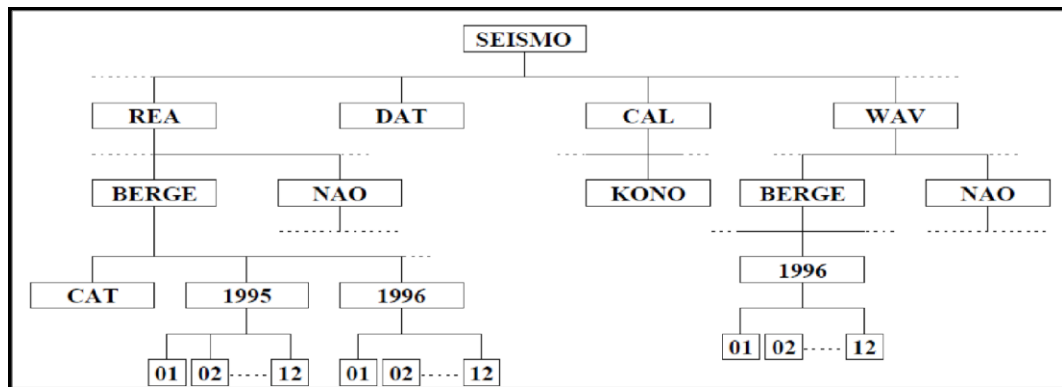


Figure 2.1. Structure of SEISAN (Ottemöller *et al.*, 2011).

Here, detail information about the directories that are presented in Table 2.1 is reported.

Table 2.1. The Structure of SEISAN contains the following main subdirectories.

REA: Earthquake readings and full epicenter solutions in a database
WOR: The users work directory, initially empty
TMP: Temporal storage of files, initially empty
PRO: Programs, source and executables
LIB: Libraries and subroutines in PRO and LIB
COM: Command Procedures
DAT: Default and parameterfiles, e.g. station coordinates
WAV: Digital waveform datafiles
CAL: System calibration files
INF: Documentation and information
ISO: Macroseismic information
SUP: Supplementary files and programs

2.1.2.1. Wav Directory (Waveform File Directory). In case a large number of waveform data is stored, it might be an advantage to also split up the WAV directory in subdirectories.

The WAV directory contains files with digital waveform data. The directory normally has no subdirectories or any other organization.

The analysis system always looks at WAV for particular files to check if they are properly stored in the user's own directory.

An example script is given below to create WAV folder.

Table 2.2. An example of generating a SEISAN format using WAVETOOL.

```

C:\seismo\WOR\20100508_014627>dirf *.KO
C:\seismo\WOR\20100508_014627>wavetool
Filename of s-file or waveform file, number or filenr.lis
filenr.lis
c:\seismo\WOR\20100508_014627>seisei
Merge <1> or split <2> files:
1
>Output format, seisan or mseed ?
seisan
>Give 1-5 letter network code for merged file(s), NSN is default
UDIM
Maximum difference (sec) of events to merge, return for default (180 secs)
Filename of s-file or waveform file, number or filenr.lis
Stop - Program terminated.
C:\seismo\WOR\20100424_051507>seisei
Merge (1) or split (2) files:
1
Output format, seisan or mseed ?
seisan
Give 1-5 letter network code for merged file(s), NSN is default
UDIM
Maximum difference (sec) of events to merge, return for default (180 secs)
Number. of files to merge 723.1.2
72 Number of input channels
Output file name is: 2010-04-24-0513-46S.UDIM__072 (YYYY-MM-DD-HHMM-SS-Network
Code_Station ID)
Stop - Program terminated.
C:\seismo\WOR\20100424_051507>dirf 2010-04-24-0513-46S.UDIM__072
C:\seismo\WOR\20100424_051507>mulplt
>Filename, number, filenr.lis (all), cont for cont base, conts for large SEED
1
Read headers from files:
2010-05-08-0145-11S.UDIM__064
> Plot options: Interactive picking Return
Multi trace plot on screen, def (0)
Multi trace plot on screen (1)
Multi trace plot on screen+laser(2)
Multi trace plot on laser (3)
Continuoues on screen (4)
Continuoues on screen + laser (5)
Continuoues on laser (6)
Stop (q)
0
>Low and high cut for filter, return for no filter
>ENTER EVENT TYPE L,R OR D L
Give operator code (max 4 char)
TY
>Give 2-5 letter data base, ,, for local dir, return for default base
UDIM
S-file name: 24-0513-46L.S201004
>GO AHEAD (Y/N)
Y

```

2.1.2.2. Rea Directory. The REA directory contains phase readings and derived source information like hypocenters, fault plane solutions, etc. The REA directory has one or several sub-directories corresponding to separate databases.

For quick reference and interactive work the events are shared in single files (S-files) in directories with sorted yearly and sub-directories with sorted monthly. When new data is entered into the database, it is stored as individual event files. Each S-file contains original phase readings in the nordic format which includes file names of all corresponding waveform files (See Table 2.3).

Table 2.3. A Typical S-file.

```

2010 329 0803 18.6 L TES 7 1
ACTION:UPD 14-01-28 15:44 OP:TY STATUS: ID:20100329080318 I
2010-03-29-0802-33S.udim__039 6
STAT SP IPHASW D HRMM SECON CODA AMPLIT PERI AZIMU VELO AIN AR TRES W DIS
CAZ7
BNGB BE ES 8 3 35.26 100
BNGB BN IAML 8 3 35.95 432.8 0.36
BNGB BN ES 8 3 36.17 100

```

The first line is the header with origin time, location and magnitudes, in this case 2 magnitudes. The second line gives the event ID. The third line gives the name of associated waveform files. The fourth line contains header of phase lines.

The S-files are used as input for location and when making a permanent update, also for output. Events are classified either as L, R or D for local, regional or distant event respectively. This information is given in the header line of the S-file as well as in the S-file name.

2.1.2.3. Cal Directory (Response File Directory). Seisan can use either SEISAN response file format or GSE response file format that is the instrumental response which is presented as GSE response file format. Below is an example of generating a GSE response file using RESP.

Table 2.4. An example of GSE response file generated by RESP for the SEISAN.

```

RESP - PROGRAM TO CREATE RESPONSE FILES IN SEISAN
OR GSE FORMAT. THE RESPONSE CAN BE CREATED
AS POLES AND ZEROS (PAZ) OR FREQUENCY
AMPLITUDE AND PHASE (FAP). THE SAME
TRANSFER FUNCTION AND FILTERS ARE USED
IN BOTH CASES.
CHOOSE OUTPUT FORMAT:
0: NO OUTPUT FILE
1: SEISAN FAP
2: SEISAN PAZ
3: GSE2 FAP
4: GSE2 PAZ
4
TYPE OF SENSOR: 1: NONE
2: SEISMOMETER
3: ACCELEROMETER
2
SEISMOMETER NATURAL PERIOD ? 120
SEISMOMETER DAMPING RATIO ? 0.7
SENSOR LOADED GENERATOR CONSTANT (V/M/S OR V/G) ? 2982
INSTRUMENT TYPE FROM LIST BELOW
Akashi, 23900, BB-13V, CMG-3, CMG-3N, CMG-3T, CMG-3E, FBA-23, GS-13, GS-21, KS3600, KS360i,
KS5400, MK II, Oki, Parus2, S-13, S-500, STS-1, STS-2, TSJ-1e
CHOICE CMG-3T
RECORDING MEDIA GAIN (COUNT/V OR M/V) ? 0.3159E+06
DIGITIZER SAMPLE RATE (BEFORE POSSIBLE FIR FILTER) 50
DIGITIZER MODEL CMG-DM24
AMPLIFIER GAIN (DB) ? 1
NUMBER OF FILTERS (0-10), RETURN FOR NONE ?
FILE NAME FOR FILE WITH POLES AND ZEROS, RETURN FOR NO FILE
NUMBER OF FIR FILTER STAGES 0
FILE NAME FOR MEASURED VALUES, RETURN FOR NO FILE
GSE RESPONSE FILE (Y/N=default)? Y
Enter station code. e.g. BERGE, max 5 chars ADVT
Enter component (4 chars) e.g. SL Z
First character is type, must be one of the following:
S: Short period, L: Long period
B: Broad band, A: Accelerometer
Last character must be Z,N or E
Character 2 and 3 can be anything BH_Z
Enter date as YYYYMMDDHHMMSS, at least up to the day (e.g. 19880123):200605191300

```

Below is an example of GSE response file generated by RESP for the SEISAN.

Table 2.5. An example of GSE response file generated by RESP for the SEISAN.

```

CAL2 ADVT BH Z CMG-3T .84E-01 1. 50.00000 2006/ 5/19/12:30
PAZ2 1 V .34084710E+04 5 3 Laplace transform
-.37007960E-01 .37007960E-01
-.37007960E-01 -.37007960E-01
-.11309730E+04 .00000000E+00
-.10053100E+04 .00000000E+00
-.50265480E+03 .00000000E+00
.00000000E+00 .00000000E+00
.00000000E+00 .00000000E+00
.00000000E+00 .00000000E+00
DIG2 2 .31655590E+06 50.00000 T3Y19/A524

```

The first line gives station and sensor type. The following numbers in the first line after sensor type are gain in nm/c at reference period (1 seconds), sample rate, and date. In the second line (FAP2) gives a gain factor (1) at the output units (V for Volts). Finally, the frequency, gain and phase triplets are printed in the remaining lines of this example.

2.1.3. Definition Files

The other files which were used in SEISAN software are summarized below.

The most important files are in DAT: STATION0.HYP, SEISAN.DEF, MULPLT.DEF. You can remain almost all of your parameter files as their initial condition, but only SEISAN.DEF is changed in process.

Both the MULPLT.DEF and STATION0.HYP can also be in the working directory. Programs always search for these files at first and on a multi-user system, this enables different users to have their own setup. It also makes it possible to work with different setups by just changing directory.

2.2. ZSACWIN Software

Source parameters were computed by applying MTI method which is represented by a point source model. Focal mechanism solutions were calculated by using ZSACWIN software package. Source parameters were obtained from the inversion. In addition,

Seismic moment and fault geometry (strike ,dip, rake angles) were calculated by following Dreger 2002, Dreger and Helmberger (1993) technique.

2.2.1. Layout of ZSACWIN Software on Computer

The database of ZSACWIN consists of the ZSACWin, ZSACWork and their subdirectories that contain readings, source information and waveform data for each event.

The folder consists of executable programs and related configuration files, together with GMTmap (Generic Mapping Tools), Synthetics and SYSTEM sub folders which are stored in the root (Table 2.6).

Table 2.6. Sub index and files which are stored in the main folder.

zSacWin	Files	Folders													
		GMTmap													
	FTPandMail.exe gdaacs.ini gdaacs.txt getdat-sao-intel74.d globals.ini PNTAKOF.DAT PPTAKOF.DAT PTAKOF.DAT SMS.INI SMS.txt telsiz.ini telsiz.txt wsinfo74.d zSacWin.exe zTelsiz.exe		<table border="1"> <thead> <tr> <th>Files</th> <th>Folders</th> </tr> </thead> <tbody> <tr> <td></td> <td> bin gsdll32.dll gswin32c.exe gswin64c.exe </td> </tr> <tr> <td></td> <td> config deqMap.d dkQSTN.d dMap.d dModels.d important.txt </td> </tr> <tr> <td></td> <td> CPT blueGREEN_BRW.cpt blueGREEN_GRI.cpt blueWHITE_YEL.cpt rainbow.cpt </td> </tr> <tr> <td></td> <td> DATA bos.ras fay3.dat ilcelel.TXT iller.txt Imza.ras Topo30s.grd Topo30s_int.grd </td> </tr> <tr> <td></td> <td> Stnlist KO-OBO.TXT StnKoeniACC.txt StnKoeniBB.txt StnOthers.txt zzDeniz.txt </td> </tr> </tbody> </table>	Files	Folders		bin gsdll32.dll gswin32c.exe gswin64c.exe		config deqMap.d dkQSTN.d dMap.d dModels.d important.txt		CPT blueGREEN_BRW.cpt blueGREEN_GRI.cpt blueWHITE_YEL.cpt rainbow.cpt		DATA bos.ras fay3.dat ilcelel.TXT iller.txt Imza.ras Topo30s.grd Topo30s_int.grd		Stnlist KO-OBO.TXT StnKoeniACC.txt StnKoeniBB.txt StnOthers.txt zzDeniz.txt
Files	Folders														
	bin gsdll32.dll gswin32c.exe gswin64c.exe														
	config deqMap.d dkQSTN.d dMap.d dModels.d important.txt														
	CPT blueGREEN_BRW.cpt blueGREEN_GRI.cpt blueWHITE_YEL.cpt rainbow.cpt														
	DATA bos.ras fay3.dat ilcelel.TXT iller.txt Imza.ras Topo30s.grd Topo30s_int.grd														
	Stnlist KO-OBO.TXT StnKoeniACC.txt StnKoeniBB.txt StnOthers.txt zzDeniz.txt														
		Synthetics <table border="1"> <thead> <tr> <th>Files</th> <th>Folders</th> </tr> </thead> <tbody> <tr> <td></td> <td> 02 . syn_0010_02.hlm syn_0015_02.hlm ... syn_1200_02.hlm </td> </tr> <tr> <td></td> <td> 98 syn_0010_98.hlm syn_0015_98.hlm ... syn_1200_98.hlm </td> </tr> </tbody> </table>	Files	Folders		02 . syn_0010_02.hlm syn_0015_02.hlm ... syn_1200_02.hlm		98 syn_0010_98.hlm syn_0015_98.hlm ... syn_1200_98.hlm							
Files	Folders														
	02 . syn_0010_02.hlm syn_0015_02.hlm ... syn_1200_02.hlm														
	98 syn_0010_98.hlm syn_0015_98.hlm ... syn_1200_98.hlm														
		SYSTEM <table border="1"> <thead> <tr> <th>Files</th> <th>Folders</th> </tr> </thead> <tbody> <tr> <td> dbResponseFinal.xls inp.mdb catalog.mdb Katsay.txt Locmapq.jpg map.txt MW.mdb stnmap.jpg zQanizer.INI </td> <td> Models CrustModel.txt DoguAnadolu.hdr EgeBogalesi.hdr Hypo71.hdr Marmara.hdr StationList.txt </td> </tr> </tbody> </table>	Files	Folders	dbResponseFinal.xls inp.mdb catalog.mdb Katsay.txt Locmapq.jpg map.txt MW.mdb stnmap.jpg zQanizer.INI	Models CrustModel.txt DoguAnadolu.hdr EgeBogalesi.hdr Hypo71.hdr Marmara.hdr StationList.txt									
Files	Folders														
dbResponseFinal.xls inp.mdb catalog.mdb Katsay.txt Locmapq.jpg map.txt MW.mdb stnmap.jpg zQanizer.INI	Models CrustModel.txt DoguAnadolu.hdr EgeBogalesi.hdr Hypo71.hdr Marmara.hdr StationList.txt														

SYSTEM folder:

Inp.mdb: The main database that includes results of all earthquake analysis which are stored in this database.

MW.mdb: It is CMT catalog where MTI results are stored.

zQanalyzer.ini: It is the file that is used by the program itself and keeps program flow which save all preferences.

catalog.mdb: It is the database where all results are permanently saved.

2.2.2. Overall Program Flow, Function Capacity

In case of requirement, data can be retrieved from servers which provide real time data by using digital data records or EW & scream server to determine origin times, epicenters, magnitudes of earthquakes and fault mechanisms. After determination of indicators about earthquakes, final results can be also stored in servers. In addition to that, final results about earthquakes can be distributed by using various telecommunication tools such as SMS, radio, text-to speech.

Used Digital Data Formats: The main format which is used in the program is SAC (Seismic Analysis Code) digital format. Other seismic formats are converted to SAC format by using automated software tools.

3. DATA PROCESSING

Seismic source parameters and scaling relations were determined by using a data set of 29 earthquakes. We used records from the broad band network whose epicentral distances from the sensors vary in range of 10 - 600 km and whose earthquake magnitudes are ranging from 3.3 to 6.0 between March 8th and March 29th.

The compressed SAC waveform data were retrieved from KOERI network (<http://barbar.koeri.boun.edu.tr/sismo/zKDRS/>) via internet. Seismic stations equipped with broadband seismometers CMG-40T (30 sec), CMG-3T (120 sec and 360 sec) and CMG-3ESP (30 sec and 120 sec) were used in the study. These broadband seismometers are Guralp type and data were recorded continuously at 24-bits and 50 samples/sec by these sensors. In Figure 3.1, the map of the studied event and seismic stations which data are shown.



Figure 3.1. Map of the used seismic stations in the study. The figure was created by ZSacWin Analysis Software Package (Yilmazer, 2011).

For the inversion, two different source models are used to determine the respective fault radii and displacements for comparison and evaluation purposes: displacement spectra and MTI.

After the records were converted SEISAN format, further processing procedure such as location and estimation of the source parameters were performed by using the SEISAN (Havskov and Ottemöller, 2008) and focal mechanism parameters were computed by using ZSACWIN software package. In both software, the hypocenter locations of the selected earthquakes are computed by using the velocity model of Kalafat *et al.* (1987) and Kalafat *et al.* (1992).

3.1. Processing with SEISAN

The P and S arrival times are analyzed to obtain high-quality hypocenters and focal mechanisms. Obtained phase records which are stored in '*.S' database files are important due to including time and location data that are required to calculate spectrum parameters. Although, AUTOPICK software which is a product of SEISAN that automatically calculate P and S arrival times with respect to predetermined velocity model, sometimes initial time of phases are determined improperly. For reliability of the calculated source spectra phase readings were also analyzed by user. Epicenter solutions are determined by using HYPOCENTER program. The hypocenter program is a modified version of HYPOCENTER (Lienert *et al.*, 1986; Lienert, 1991; Lienert and Havskov, 1995). The main modifications are that it can accept more phases, locate teleseismic events and use input in Nordic format directly from the database. In the program, two layer crustal structure model which is used to analyze earthquakes is also used by UDIM to determine location of earthquake (Kalafat *et al.*, 1987). In addition coordinates of stations are adapted to the program.

The velocity input time series are integrated and FFT algorithm is applied to obtain displacement spectrum of the signal after the spectrum is corrected for instrument response and for all known path effects including average anelastic attenuation and geometrical spreading factors. The spectrum is corrected for geometrical spreading function to the distance of $1/R$ for $R \leq 100$ km, and $(100 \cdot R)^{-1/2}$ for $R \geq 100$ km for shear waves (Herrmann

and Kijko, 1983). The correction for anelastic attenuation functions which constitute the diminution factor is particularly important for getting the correct corner frequency and also source parameters. However there is no quality factor available neither reflecting the whole region nor the region-specific term. In this content, the quality factors is defined as the best approximation from the literature and the average value of anelastic attenuation of $Q_s=35\pm 3*f^{0.83}$ is used as proposed by Eyidoğan, *et al.* (1999) that took into account by inverting for Q is used for the entire Elazığ region.

The noise spectrum was plotted within the same figure in order to suggest comparison between signals to noise ratio before performing the inversion. The computation which was undertaken as the signal spectrum is at least 2.5 times the noise spectrum. In the case of weak signals, the data were excluded from the computations. The window length was defined as a duration of 5 seconds, which starts 1 sec before the S wave onset for all computations. As a final step, the magnitude M_w was computed out of the seismic moment in parallel to empirical relation that was proposed by Hanks and Kanamori (1979).

The corrected spectra were scaled to compute moment at the long period asymptote which is corresponding to the spectra plateau. Using the spectral amplitude (Ω_0) for 0 Hz, M_0 and f_c which control the shape of the spectra were derived from the fitted model based on the Brune's ω^{-2} source model. Source parameters and moment magnitudes of earthquakes are determined by fitting this spectrum to classical Brune's ω^{-2} source model. With respect to this aim, an automatic routine named as AUTOSIG which is developed by Ottemöller and Havskov (2003) was utilized based on minimizing the differences between observed and synthetic source spectra identified by the S waves.

The fitting combination of these parameters is obtained by applying the CGS technique that requires several iterations from an initial model condition. In this technique, the model space is partitioned into grid structure and the error function is identified for all grid points. The best solution through iterative procedure is obtained when iteration reaches a smaller grid with denser spacing around the expected best solution (Ottemöller and Havskov, 2003). The best fitting iteration of the parameters is obtained after a few seconds. As a final step, the magnitude M_w is computed as an output of the seismic moment calculation procedure (Hanks and Kanamori 1979).

3.2. Processing with ZSACWIN

ZSacWIN software program developed by Yilmazer (2013) helps real time assessment of received digital seismological data to the processing center. It is compatible with Windows operating systems. In the program presetting, some routines utilizes from SAC, SEISAN, Numerical Recipes, Earthworm, HYPO71, FKPROG and TDMT_INVC software packages. While the program provides fully automated process, it also allows user to intervene at any step of process. Furthermore, the program allows user to run the process several times by using various parameters.

The analysis of the dataset which consists of 29 earthquake records with magnitude ranging from 3.3 to 6.0 is done by using ZsacWin software program. In this context, all parameters of each earthquake (longitute, latitude, depth and magnitude) are calculated by using ZsacWin software program. In addition, faulting mechanisms for each earthquake are determined by using MTI method.

In the study, horizontally layered crustal model (Kalafat *et al.*, 1992) that is a model also used by UDIM to determine earthquake location is used to analyze earthquakes.

Table 3.1. Velocity structure ($V_p/V_s=1.73$).

P wave velocity -Vp (km/s)	Depth (km)
4.50	00.00
5.91	05.04
7.80	31.60
8.30	69.20

3.2.1. Generalized Processing Structure of ZSacWin

In waveform data processing, the software consists of three main sections. The first section of the software is used to visualize waveform data on screen to apply various operations like filtering, phase picking etc. In the second section, origin time, event location and magnitude of earthquake are determined using phase reading that was picked on the previous stage. In last section, the software calculates earthquake faulting parameters (seismic moment, strike, dip and rake angles) using MTI method (Figure 3.2).

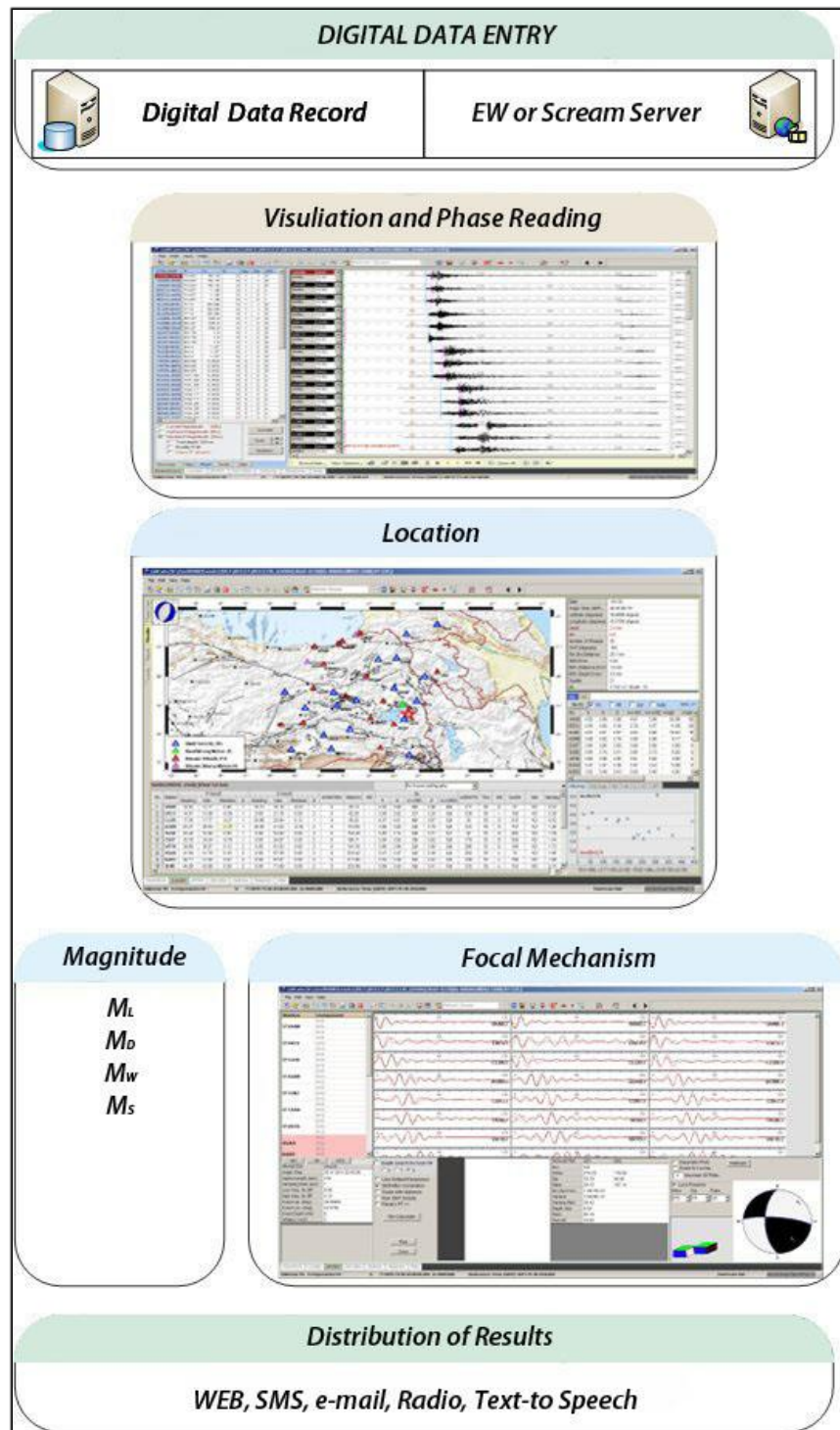


Figure 3.2. Flow diagram related to main functions of the software.

3.2.2. Determination of Epicenter and Origin Time of Earthquakes

ZsacWin software uses HYPO71 (Lee and Lahr, 1972) based location routines to determine coordinates, depth and origin time of an earthquake. Input files of location subroutines are automatically generated by using previously created crust model files, station information file and phase readings.

3.2.3. Determining Magnitude of an Earthquake

The software calculates following four different magnitudes according to predefined conditions; duration magnitude (M_D), local magnitude (M_L), moment magnitude (M_w) and surface wave magnitude (M_S). In this work, only M_L and M_w magnitudes are taken into account.

3.2.3.1. Local Magnitude. Generalized formula of local magnitude is

$$M_L = \log_{10}A + \log_{10}A_0(\Delta) \quad (3.1)$$

Here M_L is local Magnitude, A is maximum gain (micron), A_0 is maximum gain for reference earthquake (micron), Δ is distance from epicenter (km). In this study, $\log_{10}A_0(\Delta)$ expression are defined as following equations depending on epicenter distances (Görgün, 2003).

$$M_L = \log_{10}A + 0.0334\Delta - 1.9236E-4 \Delta^2 + 4.0224 \Delta^3 + 1.265, \quad (\Delta \leq 200) \quad (3.2a)$$

$$M_L = \log_{10}A + 0.0082\Delta - 5.9628E-6 \Delta^2 + 2.1173, \quad (200 > \Delta) \quad (3.2b)$$

Moment magnitude formula used in ZsacWin software is

$$M_w = 2/3 \log_{10}(M_0) - 10.73 \quad (3.3)$$

where, M_w is moment magnitude, M_o is seismic moment (dyne-cm) (results of MTI) (Hanks and Kanamori, 1979).

3.2.4. Determination of Faulting Parameters Using MTI

The software uses two different methods to determine faulting mechanism; the first is motion directions (Suetsugu, 1998) and the second is MTI (Dreger, 2002). In this research, MTI (Dreger, 2002) method is preferred.

Basic requirements of MTI method are pre-calculated Green's functions (synthetic seismograms) and SAC formatted waveform seismic data. Other inputs (latitude, longitude, depth, and origin time) are automatically gathered from previous calculations. Frequency range for band-pass filtering is also selected automatically by the software based on M_L magnitude which is calculated before.

The general representation of seismic sources is simplified by considering both a spatial and temporal point source.

$$U_n(x,t) = M_{ij}(z,t) \cdot G_{ni,j}(x,z,t) \quad (3.4)$$

U_n is displacement (the observed n^{th} station), $G_{ni,j}$ is Green's function of n^{th} station, M_{ij} is the scalar seismic moment tensor. x is distance from the source to the station, z is depth of the source and i,j are geographic coordinates.

In abovementioned equality, U (displacement) defines observed input while G is synthetic input that defines characteristics of the given crust model. Therefore, determination of the moment tensor components which provide the best consistency between these two inputs is the essence of this method. In the implemented method, it is assumed that the best consistency is reached at the value when variance reduction (VR) Equation (3.5) is maximized.

$$VR = \left\{ 1 - \sum_i \left[\frac{\sqrt{(data_i - synth_i)^2}}{\sqrt{data_i^2}} \right] \right\} \cdot 100 \quad (3.5)$$

where *data*, and *synth* are the data and Green's function time series, respectively.

Relations between scalar moment tensor components (M_{ij}), seismic moment (M_0) and faulting parameters are shown in Table 3.2 and for a double-couple point source, a sample output of MTI results for the earthquake at 07:47:38 on 2010.08.03 in Elazığ - Kovancılar ($M_L=5.6$, $M_w=5.5$) is presented in Figure 3.3.

Table 3.2. Relations between scalar moment tensor components (M_{ij}), seismic moment (M_0) and faulting components (strike, dip and rake).

In this equation, M_0 is defined as seismic moment. Components related to geographic coordinates are determined as below:

$$M = \begin{bmatrix} M_{xx} & M_{xy} & M_{xz} \\ M_{yx} & M_{yy} & M_{yz} \\ M_{zx} & M_{zy} & M_{zz} \end{bmatrix} \quad \begin{aligned} M_{xx} &= -M_0 [\sin(\delta) \cos(\lambda) \sin(2\phi) + \sin(2\delta) \sin(\lambda) \sin^2(\phi)] \\ M_{xy} &= M_0 [\sin(\delta) \cos(\lambda) \cos(2\phi) + 0.5 \sin(2\delta) \sin(\lambda) \sin(2\phi)] \\ M_{xz} &= -M_0 [\cos(\delta) \cos(\lambda) \cos(\phi) + \cos(2\delta) \sin(\lambda) \sin(\phi)] \\ M_{yy} &= M_0 [\sin(\delta) \cos(\lambda) \sin(2\phi) - \sin(2\delta) \sin(\lambda) \cos^2(\phi)] \\ M_{yx} &= -M_0 [\cos(\delta) \cos(\lambda) \sin(\phi) - \cos(2\delta) \sin(\lambda) \cos(\phi)] \\ M_{zz} &= M_0 [\sin(2\delta) \sin(\lambda)] = -(M_{xx} + M_{yy}) \end{aligned}$$

δ : (dip), the angle between fault plane and surface (horizontal).
 ϕ : (strike) the angle between fault direction and geographic north.
 λ : (rake) the angle between slip vector and fault direction.

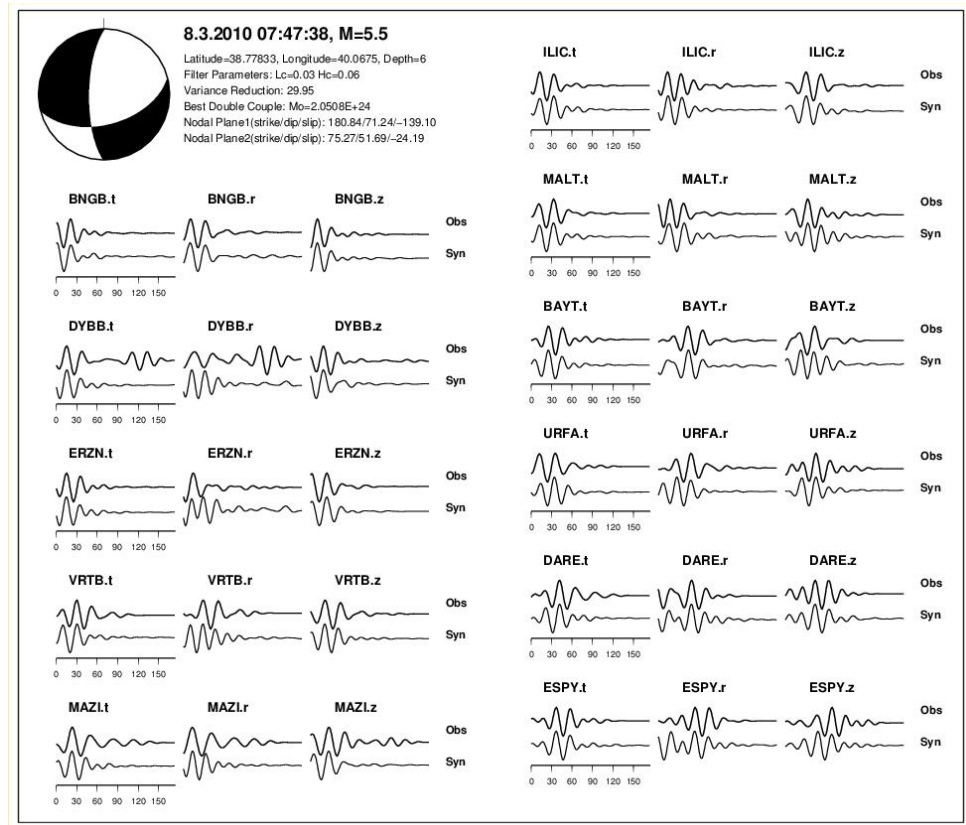


Figure 3.3. MTI results for 2010.08.03 07:47:38 Elazığ - Kovancılar earthquake.

4. RESULTS

The average source parameters and source model for 29 moderate to large size aftershocks of the 2010 Elazığ seismic event are analyzed in this section. Under scope of this study, two different source models, which are namely displacement spectra and MTI, are used to determine the respective fault radii and displacements for comparison and evaluation purposes.

The source parameters namely as; the moment magnitude, seismic moment, spectral level of corner frequency, stress drop, and fault dimension calculations are computed using displacement spectra after correcting the S-waves for instrument and the whole path attenuation (Table 4.1). Then, source parameters of the modified data are determined by using Brune's ω^{-2} source model. Earthquake source parameters and the moment magnitude, M_w are mean values that are computed by using estimated parameters of respective stations. Figure 4.1 demonstrates a graphical representation of correlation and observed displacement spectra for event #1 which is given in the Table 4.1 that recorded at MAZI, MALT, BNN and BAYT stations. The blue line presents the original displacement spectrum; the red line indicates the synthetic spectrum resulted from the automatic procedure; the green line at the bottom signs the noise spectrum taken from the signal before the first P phase arrival. Examples of displacement source spectra for event #10 which is given in the Table 4.1 that recorded at AGRB, DYBB, BNN and BAYT stations. are shown in Figure 4.2. Examples of displacement source spectra for event #29 which is given in the Table 4.1 that recorded at BNGB, DYBB, ILIC and PTK stations are demonstrated in Figure 4.3.

Table 4.1. Estimated source parameters of 29 earthquakes which are given with their mean values and standard deviations. In order, N: event ID, Date: year, month, day, Hour: hour and minutes of origin time (UTC), h: depth (km), M_L : the Richter magnitude, M_w : the mean value of stations moment magnitude, Std: standard deviation of given value, M_o : seismic moment (dyne-cm), σ : stress drop in bars, f_c : corner frequency, α : source radius in km, GAP: maximum azimuthal gap between stations used in location, NS: number of stations used in solutions, respectively.

N	Date	Hour	Lat °N	Lon °E	h (km)	M_L	M_w^{spec}	M_w^{spec} ±Std	M_o	M_o ±Std	σ	f_c	f_c ±Std	α	GAP	NS
1	20100308	02:32	38.833	40.163	5.0	6.0	6.0	0.1	1.80E+25	0.1	60.7	0.3	0.1	6.316	41	4
2	20100308	03:20	38.854	40.189	3.0	4.1	4.1	2.4	1.52E+22	8.8	26.4	1.7	1.1	1.011	52	9
3	20100308	07:47	38.777	40.113	5.0	5.5	5.4	1.6	1.72E+24	5.0	41.6	0.4	0.2	3.166	45	12
4	20100308	08:06	38.800	40.086	2.0	3.8	3.7	2.4	1.47E+21	9.3	17.0	2.3	1.5	0.572	124	5
5	20100308	08:11	38.764	40.046	2.0	4.3	4.3	2.9	1.56E+22	10.4	37.4	1.2	0.9	1.416	78	9
6	20100308	08:16	38.785	40.144	5.0	3.4	3.6	3.1	1.44E+21	12.5	19.1	2.8	2.5	0.470	81	4
7	20100308	09:00	38.782	40.119	5.0	4.8	4.7	2.3	1.61E+23	8.0	28.3	0.9	0.6	1.651	51	12
8	20100308	09:21	38.795	40.070	2.0	3.5	3.6	0.0	1.45E+21	0.0	19.1	2.7	0.0	0.470	174	1
9	20100308	09:30	38.880	40.229	5.0	3.7	3.7	2.6	1.47E+21	10.4	24.6	2.3	1.8	0.901	60	6
10	20100308	10:14	38.836	40.200	5.0	5.1	4.8	1.7	1.63E+23	5.6	34.6	0.8	0.4	1.931	51	17
11	20100308	11:12	38.764	40.138	5.0	5.3	4.8	2.6	1.63E+23	8.9	36.3	0.8	0.6	1.804	55	17
12	20100308	12:50	38.847	40.173	5.0	3.2	3.5	2.3	1.43E+21	9.6	14.3	2.6	2.1	0.624	59	9
13	20100308	14:17	38.782	40.124	3.6	4.1	4.0	1.8	1.51E+22	6.8	12.5	1.4	1.0	1.111	51	5
14	20100308	15:04	38.770	40.109	5.0	4.7	4.6	1.9	1.60E+23	6.5	18.5	0.9	0.5	1.599	48	6
15	20100309	00:09	38.770	40.095	5.0	4.0	4.0	2.8	1.51E+22	10.6	26.3	2.0	1.5	0.639	53	4
16	20100309	06:14	38.806	40.116	5.0	4.2	4.0	2.9	1.52E+22	10.7	4.3	1.0	0.7	1.565	86	4
17	20100309	07:21	38.869	40.249	5.0	4.2	4.0	2.8	1.51E+22	10.7	27.2	2.1	1.6	0.642	52	4
18	20100309	07:34	38.763	40.120	5.0	4.1	4.1	2.7	1.53E+22	10.0	10.2	1.3	1.0	1.190	51	7
19	20100309	17:10	38.747	40.051	5.0	3.5	3.9	0.0	1.49E+22	0.0	1.8	1.0	0.0	1.273	136	1
20	20100311	06:30	38.806	40.131	5.0	3.5	3.9	2.5	1.49E+22	9.7	24.8	2.4	1.9	0.626	53	7
21	20100311	09:02	38.813	40.165	5.0	3.6	3.7	2.3	1.46E+21	9.2	8.0	2.0	1.5	0.718	69	5
22	20100312	01:35	38.743	40.103	5.0	3.6	3.7	2.8	1.46E+21	11.1	74.6	3.3	2.5	0.466	88	7
23	20100312	22:50	38.838	40.094	3.8	3.8	3.7	2.6	1.46E+21	10.3	38.5	2.7	1.9	0.804	96	4
24	20100316	09:33	38.593	39.707	6.5	3.8	3.8	2.2	1.48E+21	8.5	11.0	1.9	1.3	0.887	90	6
25	20100318	02:58	38.646	39.688	5.0	3.6	3.5	2.7	1.44E+21	10.9	9.0	2.2	1.8	0.690	64	7
26	20100318	13:46	38.823	40.051	6.5	3.5	3.4	2.8	1.41E+21	11.5	44.2	4.4	3.8	0.362	89	6
27	20100320	11:22	38.767	40.038	5.0	3.5	3.3	2.3	1.41E+21	9.9	14.6	3.9	2.8	0.327	100	2
28	20100324	14:11	38.837	40.177	5.0	5.1	4.8	3.1	1.62E+23	10.6	18.3	0.7	0.5	2.448	122	7
29	20100329	08:03	38.839	40.111	7.0	3.3	3.3	2.3	1.40E+21	9.9	8.5	3.3	2.4	0.407	97	4

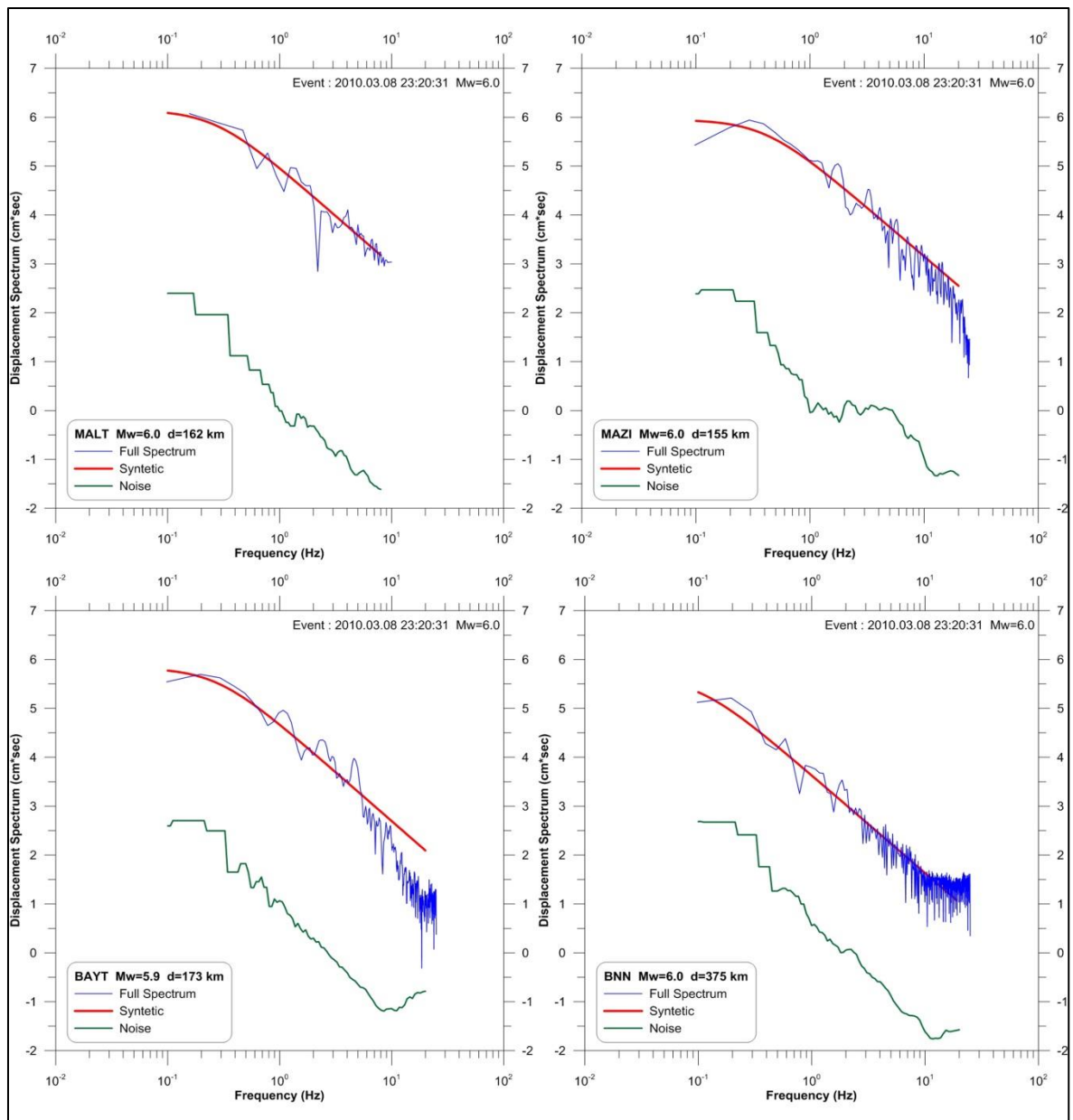


Figure 4.1. Examples of displacement source spectra obtained for event #1 (see Table 4.1). The blue line presents the original displacement spectra; the red line indicates the synthetic spectra resulted from the automatic procedure; the green line at the bottom signs the noise spectra.

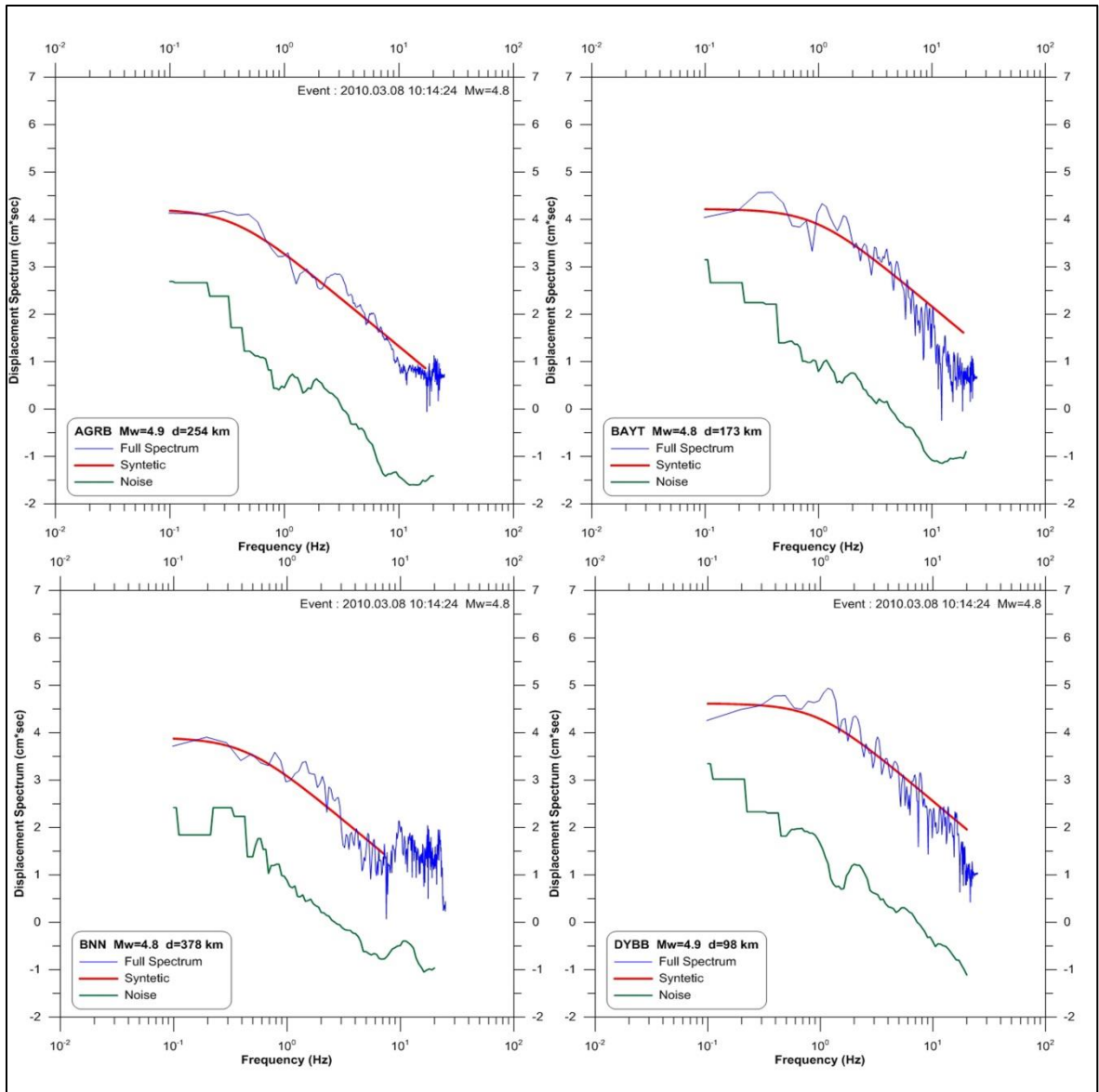


Figure 4.2. Examples of displacement source spectra for event #10 (see Table 4.1). The blue line presents the original displacement spectra; the red line indicates the synthetic spectra resulted from the automatic procedure; the green line at the bottom signs the noise spectra.

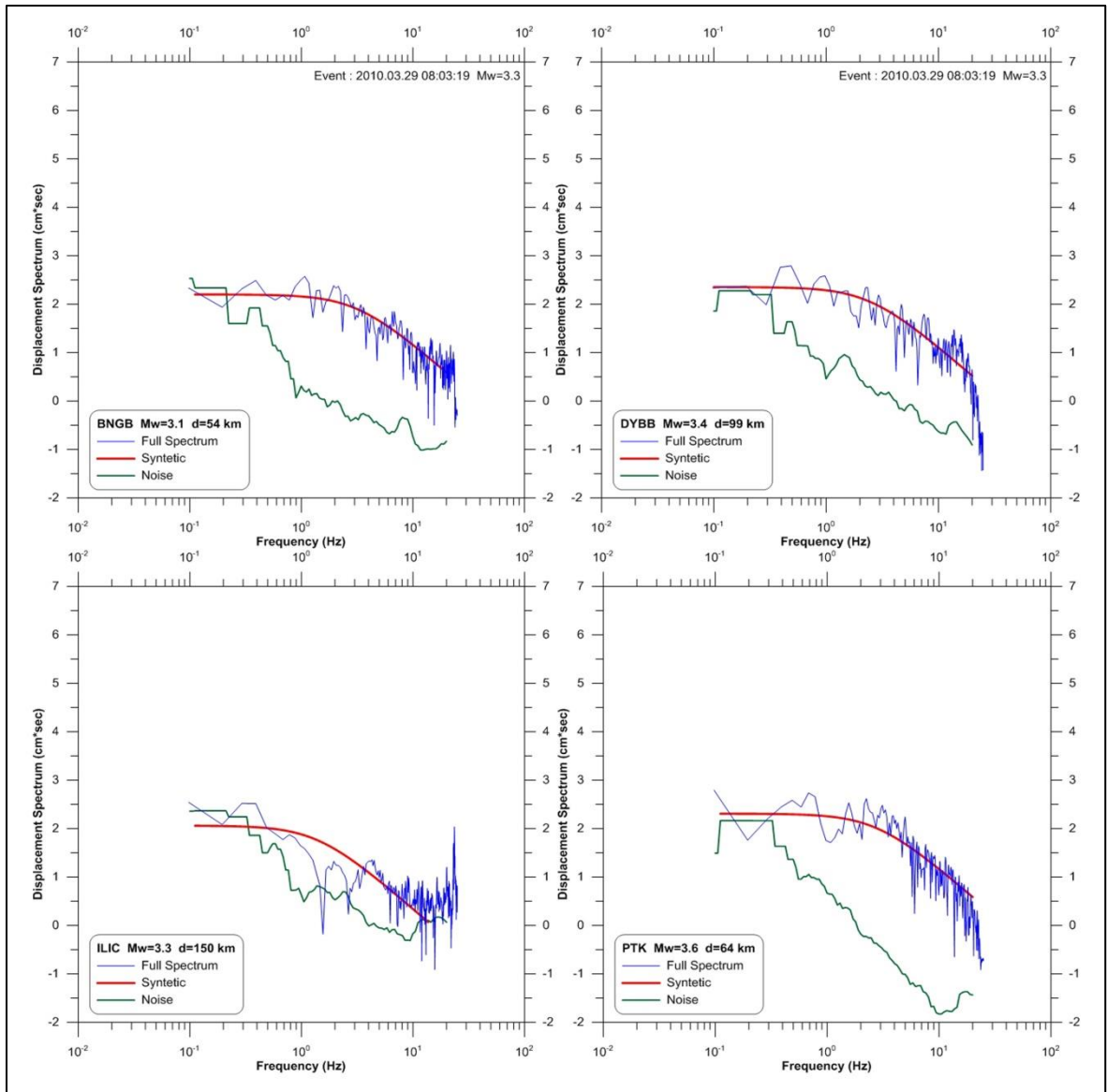


Figure 4.3. Examples of displacement source spectra for event #29 (see Table 4.1). The blue line presents the original displacement spectra; the red line indicates the synthetic spectra resulted from the automatic procedure; the green line at the bottom signs the noise spectra.

The estimated M_w results taken from displacement spectra are compared with previously determined M_L results taken from KOERI's catalogue (Figure 4.4).

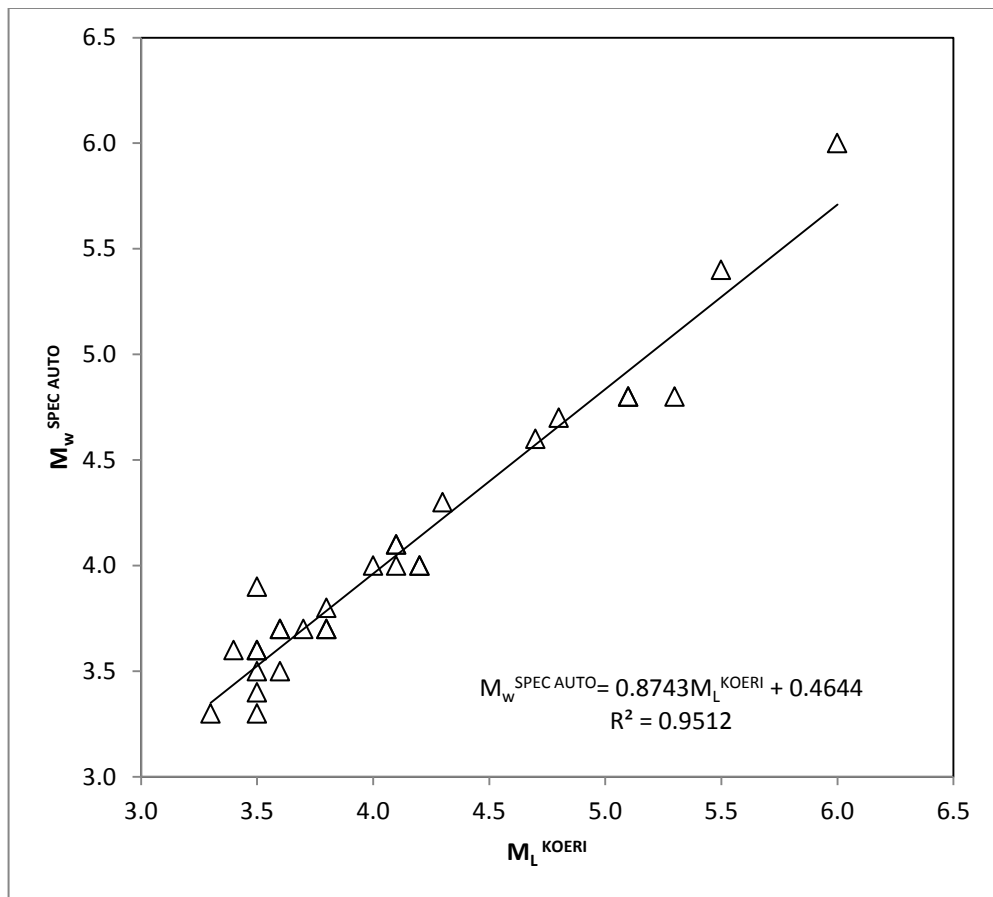


Figure 4.4. Comparison of the spectral M_w results versus M_L results taken by the KOERI's catalogue.

The magnitude results of 29 events indicate consistency with results of source parameters. Figure 4.5 shows the comparison of computed results of the scaling relationship of moment magnitude and the corner frequency. The trend in the figure suggests a nonlinear negative relationship between these two parameters. In more detail, the corner frequency decreases with declining increments when M_w magnitude increases. This trend is theoretically expected. Additionally, the seismic moment (M_o) was plotted versus the source radius (α) that suggests the source radius values increase with M_o (Figure 4.6).

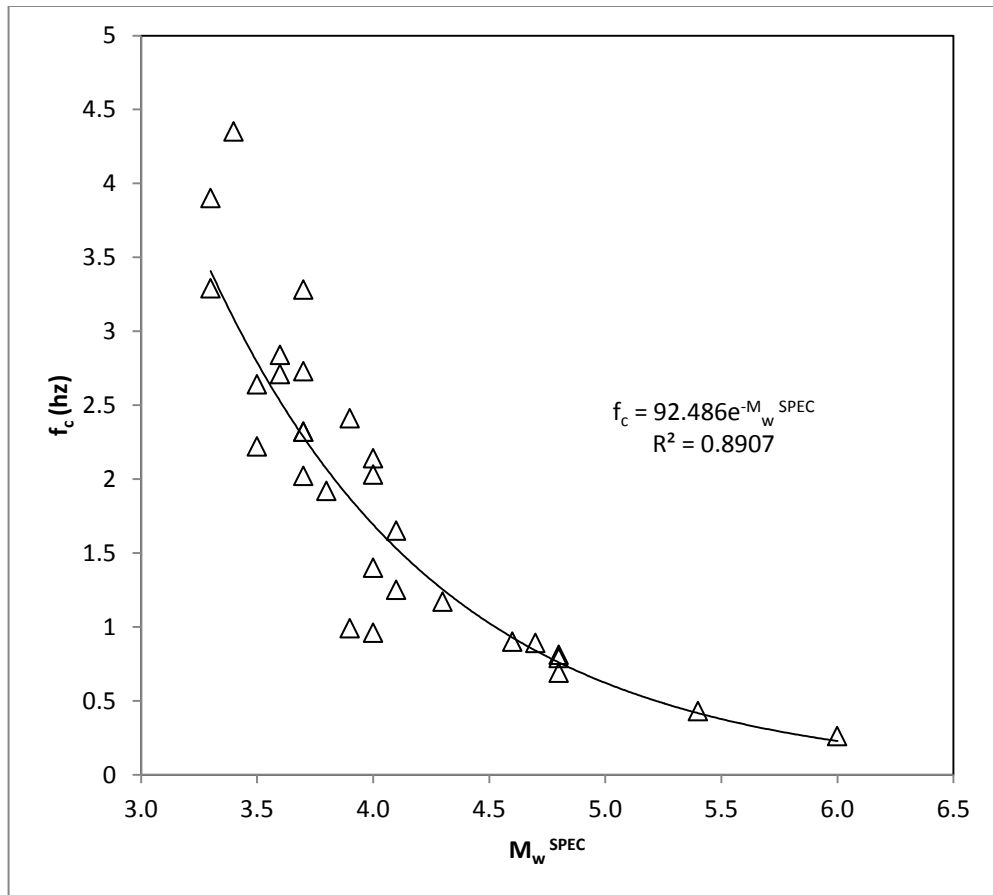


Figure 4.5. Comparison of the estimated parameters with the scalings Moment Magnitude of as a function of corner frequency.

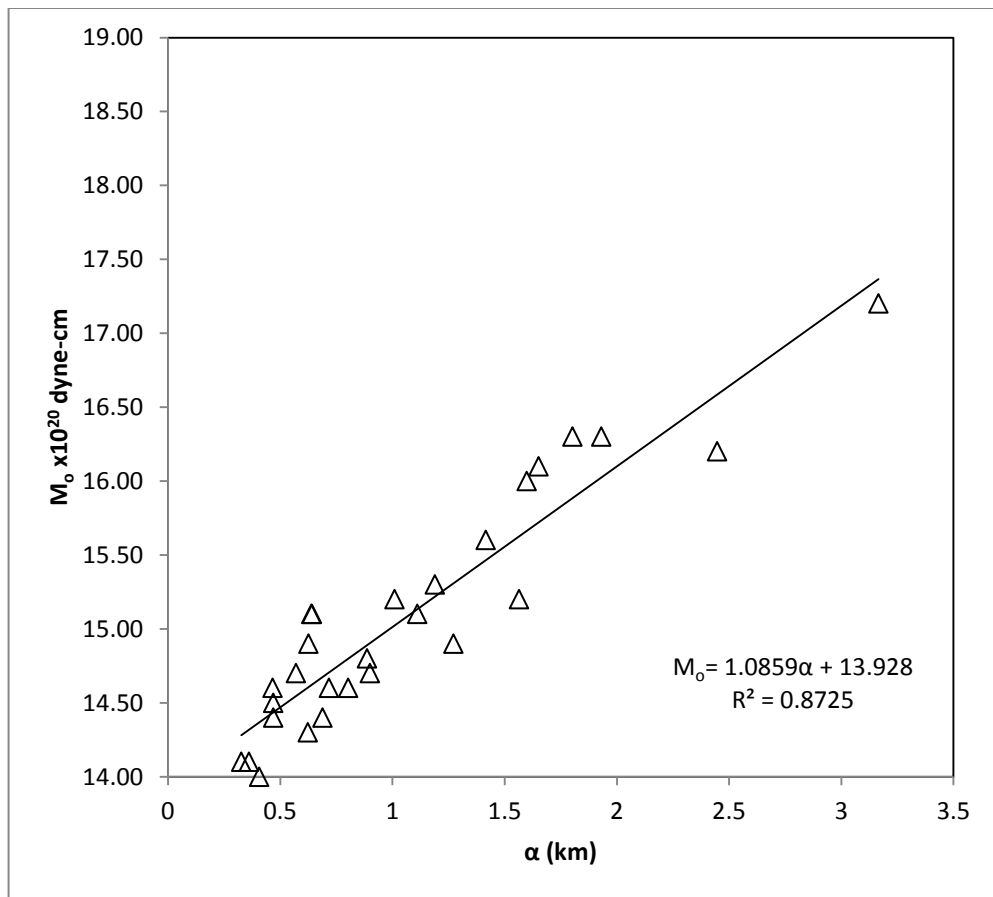


Figure 4.6. The estimated parameters based on source radius as a function of seismic moment.

As a second inversion; MTI is used to obtain source fault parameters (strike, dip, and rake), and seismic moment (Table 4.2). To this extend, information regarding movement size and magnitude of the source are obtained by using ZSACWin software. The computed solutions using MTI method are depicted in Figure 4.7.

Table 4.2. Obtained source fault parameters and seismic moment with using MTI method.

N	Origin Time	Lat °N	Lon °E	depth (km)	Str. (°)	Dip(°)	Rake (°)	Str. (°)	Dip (°)	Rake (°)	Mw	Mo
1	20100308_023231	38.82667	40.12833	12	154.20	76.30	-157.35	58.55	68.03	-14.80	5.9	7.21E+24
2	20100308_032023	38.82233	40.16633	6	197.38	68.82	-41.77	305.27	51.6	-153	4.1	1.45E+22
3	20100308_074738	38.77833	40.06750	6	180.84	71.24	-139.1	75.27	51.69	-24	5.5	2.05E+24
4	20100308_080607	38.78300	40.08700	4	124.22	84.42	171.25	215.08	81.29	5.65	3.9	8.52E+21
5	20100308_081120	38.76050	40.06116	6	135.39	68.22	143.02	241	56.04	26.6	4.2	2.08E+22
6	20100308_081620	38.77934	40.06767	6	107.97	73.99	146.5	208.32	57.96	19	3.6	2.55E+21
7	20100308_090045	38.75867	40.08000	6	288.58	51.31	70.27	138.42	42.72	113	5.2	6.29E+23
8	20100308_092158	38.81650	40.10017	6	224.37	82.97	29.63	130.39	60.61	172	3.3	1.09E+21
9	20100308_093004	38.85966	40.17800	6	283.46	69.74	-149.49	181.92	61.56	-23	3.5	2.19E+21
10	20100308_101423	38.82917	40.12533	6	223.4	72.36	54.24	110.58	39.34	151	4.7	1.33E+23
11	20100308_111210	38.78683	40.10200	6	331.44	64.1	-60.53	99.14	38.45	-135	5.5	1.86E+24
12	20100308_125040	38.84417	40.15683	4	356.67	88.28	176.88	86.76	86.88	1.73	3.4	1.25E+21
13	20100308_141735	38.74100	40.14650	4	47.57	77.51	-47.34	150.78	44.11	-162	3.9	8.32E+21
14	20100308_150450	38.77467	40.04900	6	137.97	64.93	132.73	252.62	48.29	34.6	4.5	5.71E+22
15	20100309_000918	38.75000	40.08883	6	147.31	81.29	164.16	239.77	74.35	9.04	3.8	6.13E+21
16	20100309_061456	38.73917	40.12550	6	337.88	70.88	-141.53	233.29	54	-24	4.0	1.04E+22
17	20100309_072123	38.87933	40.21633	6	155.57	89.78	162.02	245.64	72.02	0.23	4.0	9.99E+21
18	20100309_073435	38.77200	40.13617	6	347.11	63.3	-138.99	235.77	54.11	-34	3.9	6.75E+21
19	20100309_171039	38.71783	40.01700	6	239.8	78.99	-84.1	31.39	12.48	-118	3.1	5.84E+20
20	20100311_063048	38.78383	40.09250	6	153.08	81.14	149.55	248.25	59.95	10.3	3.6	2.78E+21
21	20100311_090243	38.80333	40.11250	6	347.98	69.85	-129.61	235.37	43.68	-30	3.4	1.45E+21
22	20100312_013512	38.72467	40.10850	6	32.7	61.51	-68.74	173.5	35.01	-124	3.3	1.03E+21
23	20100312_225044	38.78183	40.07200	4	220.81	71.12	-29.15	321.04	62.56	-159	3.5	1.73E+21
24	20100316_093327	38.66067	39.73867	6	172.52	64.63	35.41	65.59	58.43	150	3.7	3.87E+21
25	20100318_025836	38.65117	39.70700	6	329.66	67.67	-148.9	226.75	61.46	-26	3.3	9.07E+20
26	20100318_134610	38.78867	40.08600	6	42.26	74.48	-26.99	140.02	64.07	-163	3.1	4.62E+20
27	20100320_112249	38.75150	40.03583	6	231.58	79.8	-11.15	323.58	79.03	-170	3.2	8.24E+20
28	20100324_141130	38.77900	40.10883	6	8.69	75.1	-91.59	194.86	14.99	-84	5.4	1.50E+24
29	20100329_080318	38.81683	40.12950	8	54.52	81.82	56.72	312.3	34.16	165	3.1	4.91E+20

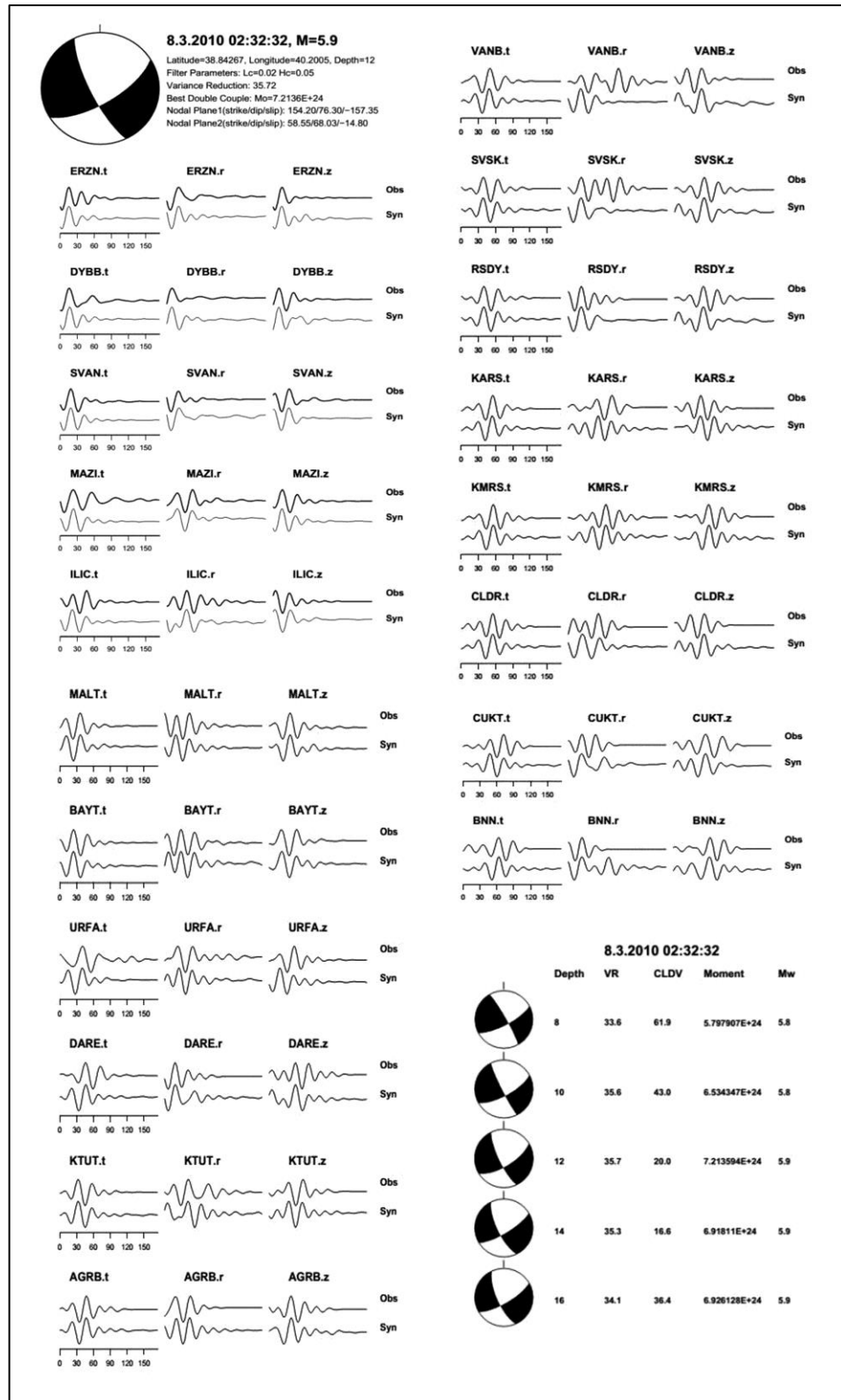


Figure 4.7. Examples of MTI method using ZSACWin software package obtained from 19 stations for event #1 (see Table 4.1).

For the verification purposes, the M_w results from displacement spectra for 29 earthquakes with magnitude ranging from 3.3 to 6.0 are compared with estimates of M_w from MTI solutions (Table 4.3). The results display that reference magnitude solutions do not differ significantly from estimates which are determined from the spectrum and the maximum difference in both of the magnitude units is found as ± 0.5 (Figure 4.8).

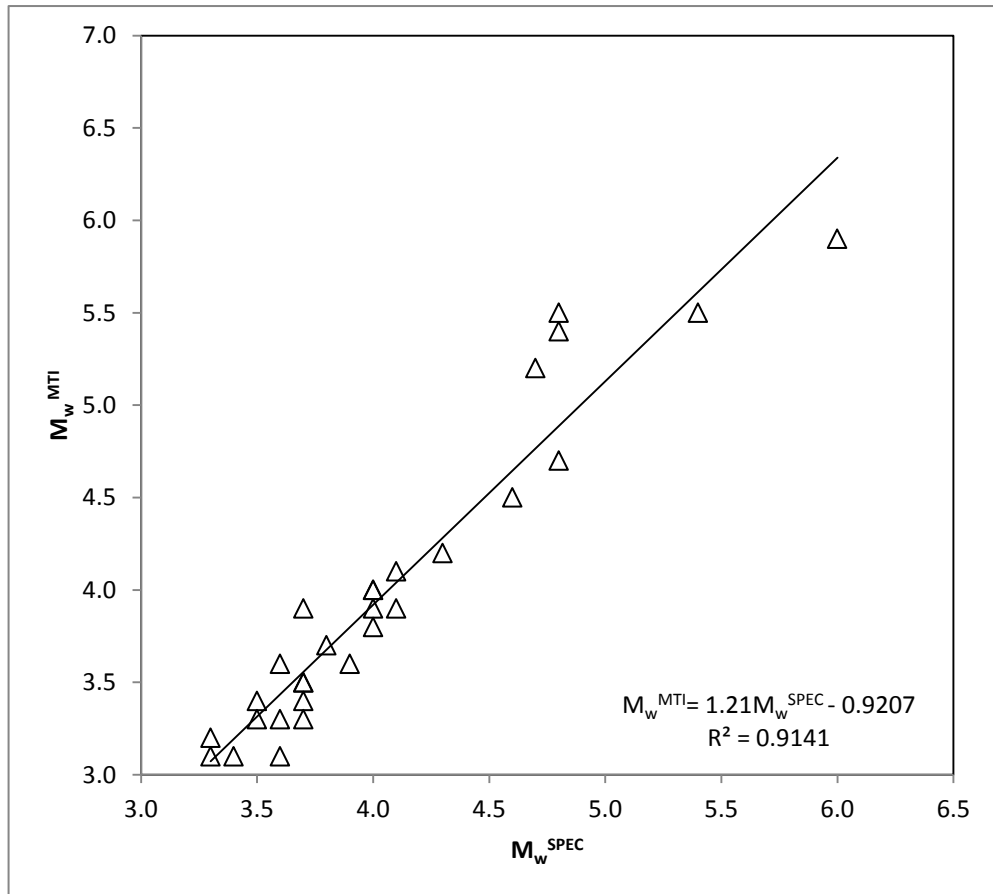


Figure 4.8. M_w^{MTI} versus M_w^{SPEC} .

Table 4.3. Comparison of both M_w values obtained from displacement spectra and MTI method.

N	Date	Hour	M_L^{KOERI}	M_w^{MTI}	$M_w^{SPEC}_{AUTO}$	origin time	Lat °N	Lon °E
1	20100308	0232	6.0	5.9	6.0	02:32:31.66	38.8426	40.2005
2	20100308	0320	4.4	4.1	4.1	03:20:24.94	38.8223	40.1663
3	20100308	0747	5.6	5.5	5.4	07:47:38.51	38.7783	40.0675
4	20100308	0806	3.8	3.9	3.7	08:06:08.13	38.7830	40.0870
5	20100308	0811	4.6	4.2	4.3	08:11:21.40	38.7605	40.0612
6	20100308	0816	3.4	3.6	3.6	08:16:21.55	38.7793	40.0677
7	20100308	0900	4.9	5.2	4.7	09:00:46.40	38.7587	40.0800
8	20100308	0921	3.5	3.3	3.6	09:21:59.38	38.8165	40.1002
9	20100308	0930	3.7	3.5	3.7	09:30:05.78	38.8597	40.1780
10	20100308	1014	5.2	4.7	4.8	10:14:23.48	38.8292	40.1253
11	20100308	1112	5.3	5.5	4.8	11:12:10.79	38.7868	40.1020
12	20100308	1250	3.5	3.4	3.5	12:50:40.86	38.8442	40.1568
13	20100308	1417	4.1	3.9	4.0	14:17:34.78	38.7410	40.1465
14	20100308	1504	4.7	4.5	4.6	15:04:51.36	38.7747	40.0490
15	20100309	0009	4.0	3.8	4.0	00:09:18.81	38.7500	40.0888
16	20100309	0614	4.2	4.0	4.0	06:14:57.00	38.7392	40.1255
17	20100309	0721	4.2	4.0	4.0	07:21:23.72	38.8793	40.2163
18	20100309	0734	4.1	3.9	4.1	07:34:35.60	38.7720	40.1362
19	20100309	1710	3.5	3.1	3.6	17:10:39.49	38.7178	40.0170
20	20100311	0630	3.5	3.6	3.9	06:30:48.90	38.7838	40.0925
21	20100311	0902	3.6	3.4	3.7	09:02:43.88	38.8033	40.1125
22	20100312	0135	3.6	3.3	3.7	01:35:12.71	38.7247	40.1085
23	20100312	2250	3.8	3.5	3.7	22:50:44.67	38.7818	40.0720
24	20100316	0933	3.8	3.7	3.8	09:33:27.50	38.6607	39.7387
25	20100318	0258	3.6	3.3	3.5	02:58:37.42	38.6512	39.7070
26	20100318	1346	3.5	3.1	3.4	13:46:10.16	38.7887	40.0860
27	20100320	1122	3.5	3.2	3.3	11:22:49.16	38.7515	40.0358
28	20100324	1411	5.1	5.4	4.8	14:11:30.85	38.7790	40.1088
29	20100329	0803	3.3	3.1	3.3	08:03:18.40	38.8168	40.1295

5. CONCLUSIONS

On 8 March, 2010 a $M_w=6.0$ mainshock occurred in Elazığ province, Başyurt-Karakoçan region of Turkey and followed by moderate to large earthquake sequence. The broadband network recorded a data set of 29 earthquakes whose epicentral distances are within 10 to 600 km and magnitudes are ranging from $3.3 \leq M \leq 6.0$ in the time period from March 8 to March 29, 2010 are used to determine seismic source parameters and scaling relations. In the present work the source process of these earthquakes are analyzed in terms of the focal mechanism parameters, moment magnitude, seismic moment, spectral level of corner frequency, stress drop and fault dimension calculations. In addition to computed parameters with MTI method, other parameters are also calculated such as; strike, dip and rake angles. In the inversion process, two different source models, which are displacement spectra and MTI, are used to determine the respective fault radii and displacements. The use of two different methods enables us to compare and verify computed parameters of the analyzed earthquake.

The velocity records are converted from time to frequency domain by implementing the formal fast fourier transform (FFT) algorithm that is required to obtain displacement spectrum of the signal after correcting the spectrum from instrument response and for all known path effects including average anelastic attenuation and geometrical spreading factors. The spectrum is corrected for geometrical spreading function to the distance of $1/R$ for $R \leq 100$ km, and $(100 \cdot R)^{-1/2}$ for $R \geq 100$ km for shear waves (Hermann and Kijko, 1983). The correction for anelastic attenuation functions constitute the diminution factor that is particularly important for getting the correct corner frequency and also source parameters, but there is on quality factor available neither in the whole region nor the region-specific term. In this content, the quality factors was defined as the best approximation from the literature, the average value of anelastic attenuation of $Q_s=35 \pm 3 \cdot f^{0.83}$ as proposed by Eyidoğan *et al.* (1999) was taken into account by inverting for Q has been used for the entire Elazığ region. The correction of $N(f)$ in displacement spectra method is necessary for any earthquake with a magnitude smaller than 3.0, however we excluded any earthquake less than 3.3 magnitude in this study. Therefore, the correction of $N(f)$ is not applied into our analysis procedure.

The displacement source spectra were determined by applying ω^{-2} spectral fitting procedure to classical Brune's (1970) model using SEISAN software package. The corrected spectra for S-waves within (5) sec are scaled to compute moment at the long period asymptote corresponding to the spectral plateau.

Using the spectral amplitude (Ω_0) for 0 Hz, M_0 and f_c which controls the shape of the spectra are derived from the fitted model based on the Brune's model by following CGS technique. In this technique, the model space is partitioned into grid structure and the error function is identified for all grid points. The best solution through iterative procedure is obtained when iteration reaches a smaller grid with denser spacing around the expected best solution (Ottemöller and Havskov, 2003). The source dimension over a circular fault area, the average stress drop, and the M_w are calculated in parallel to empirical relation which is proposed by Hanks and Kanamori (1979).

The source parameters for 29 events of moment magnitude are varying from 3.3 to 6.1 and they are estimated from the S-wave displacement spectra by using CGS method. The results are listed in Table 4.1. The estimated source parameters consist of seismic moment, corner frequency, stress drop, source radius and moment magnitude that are computed for each station separately, and then were averaged to give mean values of each event. The results display that reference magnitude solutions do not differ from estimated M_w values that were obtained from the spectrum. The maximum difference in both of the magnitude units are ± 0.4 .

Observed displacement spectra are virtually well adapted to the ω^{-2} source model in the entire frequency range for many waveforms. Therefore, the consistency in our estimations indicates that the estimated model parameters are appropriate for the region. In comparison of the solutions of source parameters that are computed by including various stations, it is not a significant inconsistencies observed among stations.

To verify consistencies of computed results, the M_w results for 29 earthquakes with magnitude ranging from 3.3 to 6.0 are compared with estimate of M_w from MTI solutions (Table 4.4). The results indicate that reference magnitude solutions are not significantly different from estimates which are determined from the spectrum. Also the maximum difference in both of the magnitude units was found to be ± 0.5 .

Source parameters determination for earthquakes in Elazığ considering source time function are computed MTI (represented by a point source model) and focal mechanism solutions using ZSACWIN software package. Source parameters obtained from the inversion, fault geometry (strike, dip, and rake angles), and seismic moment are calculated by implementing the technique which was used by Dreger (2002), Dreger and Helmberger (1993). According to the our computed MTI solutions of the earthquake in this research, Elazığ earthquake has a compressional axis on the strike of 58.55° , dip with 68.03° , and rake angle of -14.80° . In addition, we found that the computed focal mechanisms of 29 earthquakes are mostly strike-slip fault type, and a main shock seismic moment which is $M_0 = 7.21 \times 10^{24}$ dyne-cm and a moment magnitude (M_w) is 5.9, a focal depth which is $h=12$ km. Furthermore, by using displacement spectra method, we concluded that main shock's seismic moment is $M_0 = 1.80 \times 10^{25}$ dyne-cm and moment magnitude is $M_w = 6.0$.

As it can be seen from results of similar studies which are summarized here, are close to our estimations. Çubuk *et al.* (2011) found that seismic moment of the earthquake (M_0) is $7,81 \times 10^{24}$ dyne-cm, moment magnitude (M_w) is 5.9. They also asserted that this earthquake shows left-lateral strike slip faulting with a focal depth of 6 km. In addition, Tan *et al.* (2011) concluded that this earthquake has a compressional axis on the strike of 54° , dip with 80° , and rake angle of -10° and has a seismogenic brittle zone of about 15 km depth and they computed that this earthquake's moment magnitude (M_w) is 6.1. According to the study of Baykal *et al.* (2012), The 2010 Elazığ-Kovancılar earthquake is characterized by shallow depth rupture with high stress drop. General characteristic of whole EAFZ is indicated by left-lateral strike slip faulting.

According to findings of the Global CMT Project which was based on the Centroid Moment Tensor method, this earthquake has a compressional axis on the strike of 228° , dip with 83° and rake angle of -21° . In addition, according to Fault parameters obtained by Tan *et al.* (2011), this earthquake has a compressional axis on the strike of 54° , dip with 80° , and rake angle of -10° . Finally, Strike, dip and rake angles were determined as 48° , 79° and 2° , respectively by Çubuk *et al.* (2011).

M_w magnitude results of 29 events are consistent with results from source parameters. Within the magnitude range, the seismic moments are estimated in range 1.40×10^{25} to 1.80×10^{25} dyne-cm, stress drops on the fault are in range 1.8 to 74.6 bars,

corner frequencies from 0.26 to 4.35 Hz. The analysis also suggests that the main earthquake is characterized by shallow depth rupture with high stress drop. Finally, it is also concluded that as a result of the source effects to generate severe ground motion, this earthquake is a damaging type.

Although, NEMC's regional stations were used in this study, robust and reliable interpretations will be obtained by implementing the method on a denser network after including TUBITAK's data in future studies.

6. REFERENCES

- Abercrombie, R. E., 1997, "Near-Surface Attenuation and Site Effects from Comparison of Surface and Deep Borehole Recordings", *Bulletin of the Seismological Society of America*, Vol. 87, No. 3, pp. 731-744.
- Aki, K., 1967, "Scaling Law of Seismic Spectrum", *Journal of Geophysical Research*, Vol. 72, No. 4, p. 1217-1231.
- Aki, K., 1980, "Scattering and Attenuation of Shear Waves in The Lithosphere", *Journal of Geophysical Research*, Vol. 85, No. B11, p. 6496-6504.
- Aksu, A., T. Calon, D. Piper, S. Turgut and E. Izdar, 1992, "Architecture of Late Orogenic Quaternary Basins in Northeastern Mediterranean Sea", *Tectonophysics*, Vol. 210, p. 19-213.
- Arpat, E. and F. Saroğlu, 1972, "Some Observations and Thoughts on the East Anatolian Fault", *Bull. Miner. Res. Explor. Inst. Turkey*, Vol. 73, p. 44-50.
- Aydan, Ö, R. Ulusay and M. Miyajima, 2003, *The Bingöl Earthquake of May 1, 2003*, Tech. rep., Japan Society of Civil Engineers.
- Baykal, M., H. Miyake and T. Yokoi, 2012, "Source Model of the 2010 Elazığ Kovancılar Earthquake (M_w 6.1) for Broadband Ground Motion Simulation", *Proceedings of the 15th World Conference on Earthquake Engineering*.
- Bozkurt, E., 2001, "Neotectonics of Turkey - A Synthesis", *Geodinamica Acta*, Vol. 14, pp. 3-30.

Brune, J. N., 1970, "Tectonic Stress and the Spectra of Seismic Shear Waves from Earthquakes", *Journal of Geophysical Research*, Vol. 75, No. 26, pp. 4997-5009.

Brune, J. N., 1971, "Tectonic Stress and the Spectra of Seismic Shear Waves from Earthquakes", *Journal of Geophysical Research*, Vol. 76, No. 26, pp. 5002.

Çubuk, Y., S. Yolsal-Çevikbilen and T. Taymaz, 2011, "Source Parameters of March 8, 2010 Karakoçan (Elazığ, SE Turkey) Earthquakes: Synthesis of Time Domain Regional Moment Tensor and Teleseismic Body-Waves Inversions", *EGU General Assembly*, Vol. 13.

Dreger, D. S. and D. V. Helmberger, 1993, "Determination of Source Parameters at Regional Distances with Single Station or Sparse Network Data", *Journal of Geophysical Research*, Vol. 98, No. B5, pp. 8107-8125.

Dreger, D. and B. Woods, 2002, "Regional Distance Seismic Moment Tensors of Nuclear Explosions" *Tectonophysics*, Vol. 356, pp. 139–156.

Dreger, D. S., 2002, "Time-Domain Moment Tensor INVerse Code (TDMTINV C) Version1.1.

Eyidoğan, H. and A. Akinci, 1999, "Site Attenuation and Source Parameters on the North Anatolian Fault Zone, Eastern Turkey Estimated from the Aftershocks of 13 March 1992 Erzincan Earthquake", *Journal of Seismology*, Vol. 3, No. 4, pp. 363-373.

Görgün, E., 2003, *Calibration of Various Magnitude Scales in Turkey Using Broadband Data*, Master's Thesis, Boğaziçi University, Kandilli Observatory and Earthquake Research Institute.

Hanks, T. C. and H. Kanamori, 1979, "A Moment Magnitude Scale", *Journal of Geophysical Research: Solid Earth*, Vol. 84, No. B5, p. 2348-2350.

- Havskov, J. and L. Ottemöller, 2008, "SEISAN: The Earthquake Analysis Software for Windows, SOLARIS, LINUX and MACKINTOSH Version 8.2. Manual, Department of Earth Science, University of Bergen, Norway".
- Herrmann, R. B. and A. Kijko, 1983, "Modeling Some Empirical Vertical Component Lg Relations", *Bulletin of the Seismological Society of America*, Vol. 73, No. 1, pp. 157-171.
- Herrmann, R. B. and A. Kijko, 1980, "Short-Period Lg Magnitudes: Instrument, Attenuation, and Source Effects", *Bulletin of the Seismological Society of America*, Vol. 73, p. 1835-1850.
- Inceöz, M., O. Baykar, E. Aksoy and M. Doğru, 2006, "Measurements of Soil Gas Radon in Active Fault Systems: A Case Study along the North and East Anatolian Fault Systems in Turkey", *Radiation Measurements*, Vol. 41, No. 3, p. 349-353.
- Kalafat, D., C. Gürbüz and S. Üçer, 1987, "Batı Türkiye' de Kabuk ve Üst Manto Yapısının Araştırılması", *Deprem Araştırma Bülteni* , Vol. 59, pp. 43-64.
- Kalafat, D., M. Kara, Z. Öğütçü and G. Horasan, 1992, "Batı Anadolu'da Kabuk Yapısının Saptanması", *Deprem Araştırma Bülteni* , Vol. 70, pp. 64-89.
- Kalafat, D., C. Zülfikar, E. Vuran and Y. Kamer, 2010, *08 Mart 2010 Başyurt-Karakoçan (Elazığ) Depremi*, Tech. rep.,Boğaziçi University, Kandilli Observatory and Earthquake Research Institute.
- Koçyiğit, A. and A. Beyhan, 1998, "A New Intracontinental Transcurrent Structure: the Central Anatolian Fault Zone, Turkey", *Tectonophysics*, Vol. 284, p. 317-336.
- Kozlu, H., 1987, "Misis-Andırın Dolayının Stratigrafisi ve Yapısal Evrimi", *Proceedings of the 7th Biannual Petroleum Congress of Turkey, Ankara. UCTEA Chamber of*

Petroleum Engineers, p. 104-116, Turkish Association of Petroleum Geologists, Ankara, Turkey.

Kutanis, M., E. Işık and Ö. Bal, 2010, “Probabilistic Seismic Hazard Analysis of Eastern Anatolia Region, Turkey”, *14th European Conference On Earthquake Engineering*, Ohrid, Republic Of Macedonia.

Küsmezer, A. K., N. M. Özer, Şerif Barış, S. Üçer and L. Ottemöller, 2010, “Moment Magnitude Determination for Marmara Region Turkey Using Displacement Spectra”, *Geophysical Research Abstracts*, Vol:12, European Geosciences Union General Assembly.

Lee, W. H. K. and J. C. Lahr, 1972, HYP071: *A Computer Program for Determining Hypocenter, Magnitude, and First Motion Pattern of Local Earthquakes*, Open File Report, Tech. rep., U. S. Geological Survey.

Lienert, B. R. E., 1991, *Report on Modifications Made to Hypocenter*, Tech. rep., Institute of Solid Earth Physics, University of Bergen, Bergen, Norway.

Lienert, B. R., E. Berg and L. N. Frazer, 1986, “Hypocenter: An Earthquake Location Method Using Centered, Scaled, and Adaptively Least Squares”, *Bulletin of the Seismological Society of America*, Vol. 76, No. 3, pp. 771-783.

Lienert, B. R. and J. Havskov, 1995, “A Computer Program for Locating Earthquakes both Locally and Globally”, *Seismological Research Letters*, Vol. 66, No. 5, pp. 26-36.

Okay, A., A. Kaşlılar-Özcan, C. Imren, A. Boztepe-Güney, E. Demirbağ and Ö Kuşçu, 2000, “Active Faults and Evolving Strike-Slip Basins in the Marmara Sea, Northwest Turkey: A Multichannel Seismic Reflection Study”, *Tectonophysics*, Vol. 321, No. 2, p. 189-218.

- Ottmöller, L. and J. Havskov, 2003, "Moment Magnitude Determination for Local and Regional Earthquakes Based on Source Spectra", *Bulletin of the Seismological Society of America*, Vol. 93, No. 1, pp. 203-214.
- Ottmöller, L. and J. Havskov, 2010, *Routine Data Processing in Earthquake Seismology*, Springer.
- Ottmöller, L., P. Voss and J. Havskov, 2011, "SEISAN: The Earthquake Analysis Software, Version 9.0.1", University of Bergen, Bergen.
- Perinçek, D. and I. Çemen, 1990, "The Structural Relationship between the East Anatolian and Dead Sea Fault Zones in Southeastern Turkey", *Tectonophysics*, Vol. 172, p.331-340.
- Perinçek, D., Y. Gunay and H. Kozlu, 1987, "New Observations on Strike-Slip Faults in East and Southeast Anatolia", *7th Petroleum Congress of Turkey*, p. 89-103, UCTEA Chamber of Petroleum Engineers, Turkish Association of Petroleum Geologists, Ankara.
- Saroğlu, F., O. Emre and I. Kuşçu, 1992, *Annales Tectonicae*, chap. The East Anatolian Fault Zone of Turkey, p. 99-125, (Special Issue-Supplement to Volume VI).
- Stein, S. and M. Wysession, 2003, *An Introduction to Seismology, Earthquakes, and Earth Structure*, Blackwell Publishing.
- Singh, S. K., R. J. Apsel, J. Fried and J. N. Brune, 1982, "Spectral Attenuation of SH-Waves along the Imperial Fault", *Bulletin of the Seismological Society of America*, Vol. 72, p.2003-2016.
- Suetsugu, D., 1998, "*Practice on Source Mechanism*". IISEE Lecture Note. Tsukuba, Japan, p. 104.

Tan, O., Z. Pabuçcu, M. C. Tapirdamaz, S. Inan, S. Ergintav, H. Eyidoğan, E. Aksoy and F. Kuluöztürk, 2011, "Aftershock Study and Seismotectonic Implications of the 8 March 2010 Kovancılar (Elazığ, Turkey) Earthquake ($M_w = 6.1$)", *Seismological Research Letters*, Vol. 38, p. 11304.

Tucker, B. E., J. L., King, D. Hatzfeld and I.L. Nersesov, 1984, "Observations of Hard-Rock Site Effects", *Bulletin of the Seismological Society of America*, Vol. 74, p.121-136.

TÜBİTAK, MAM, 2010, *Mart 2010 Karakoçan (Elazığ) Depremi ($M_L=5.9$)*, http://http://www.ydbe.mam.gov.tr/DEPAR/2010_03_08_Elazig/

Yılmaz, H., S. Over and S. Ozden, 2006, "Kinematics of the East Anatolian Fault Zone between Türkoğlu (Kahramanmaraş) Çelikhan (Adıyaman), Eastern Turkey", *Earth Planets Space*, Vol. 58, p. 1463-1473.

Yılmaz, M., 2011, "ZSACWIN: The Earthquake Processing Software, Version 4.0. Boğaziçi University- KOERI", Istanbul.

Yılmaz, M., 2013, "ZSACWIN: A Rapid Earthquake Processing and Archiving System User Guide v2.0. Boğaziçi University- KOERI", Istanbul.